nature ecology & evolution

ARTICLES

https://doi.org/10.1038/s41559-018-0535-1

Ecological suicide in microbes

Christoph Ratzke[1,3*], Jonas Denk[2,3] and Jeff Gore[1*]

The growth and survival of organisms often depend on interactions between them. In many cases, these interactions are positive and caused by a cooperative modification of the environment. Examples are the cooperative breakdown of complex nutrients in microbes or the construction of elaborate architectures in social insects, in which the individual profits from the collective actions of her peers. However, organisms can similarly display negative interactions by changing the environment in ways that are detrimental for them, for example by resource depletion or the production of toxic byproducts. Here we find an extreme type of negative interactions, in which *Paenibacillus* sp. bacteria modify the environmental pH to such a degree that it leads to a rapid extinction of the whole population, a phenomenon that we call ecological suicide. Modification of the pH is more pronounced at higher population densities, and thus ecological suicide is more likely to occur with increasing bacterial density. Correspondingly, promoting bacterial growth can drive populations extinct whereas inhibiting bacterial growth by the addition of harmful substances—such as antibiotics—can rescue them. Moreover, ecological suicide can cause oscillatory dynamics, even in single-species populations. We found ecological suicide in a wide variety of microbes, suggesting that it could have an important role in microbial ecology and evolution.

Microbes not only depend on their environment but also modify it[1–4]. An important environmental parameter for microbial growth is pH, because protein and lipid membrane stability depend strongly on the pH of the environment[5,6]. Microbes have a species-dependent pH optimum at which they grow best[7,8] and an environmental pH above or below this optimum inhibits growth or can even cause cell death[9,10]. At the same time, bacteria change the environmental pH by their metabolic activities[9,11]. In this way, microbes can potentially induce pH values that are detrimental for their own growth and thus harm themselves.

Results

The soil bacteria species *Paenibacillus* sp. (most similar to *Paenibacillus tundrae*, for more information about this strain see Supplementary Information) can grow in a medium that contains 1% glucose as the main carbon source, in addition to a small amount of complex nutrients (see Methods for details). In soil, the amount of carbohydrates ranges from 0.1%[12] to 10%[13], mostly in the form of complex carbohydrates. Starting from neutral pH, we measured strong acidification of the environment to a pH of around 4 during bacterial growth due to the secretion of a variety of organic acids (Fig. 1a, Supplementary Fig. 1b). Upon reaching this low pH, the bacteria suddenly started to die, resulting in a non-monotonic growth curve (Fig. 1a), since *Paenibacillus* sp. cannot survive at low pH values (Supplementary Figs. 1a and 3). Indeed, after 24 h of incubation, we found that there were no viable cells in the culture (as measured by colony forming units (CFU) after 48 h incubation on rich medium, which may exclude cells that could grow after more than 48 h). We note that the bacterial densities that are reached in this experiments are within the range that can be found in soil[14,15] and soil has a slightly lower buffering capacity than our medium (Supplementary Fig. 2). Moreover, ecological suicide also appears on non-glycolytic substrates (such as glycerol) and complex sugars such as starch (Supplementary Fig. 1). We call this rapid population extinction due to environmental modification ecological suicide—a phenomenon that has previously been hypothesized[16,17].

The correlation between the drop of pH and the onset of death suggests that the bacteria themselves may be responsible for their eventual extinction by lowering the pH into regions in which they cannot survive. To test this idea, we added buffer to the medium to temper the pH change. The buffer indeed slows down the death process (Fig. 1b) and prevents it completely at sufficiently high concentrations (Fig. 1c). Thus, it is the pH change that causes the death of the bacteria and the presence of buffer can hinder ecological suicide. These results show that initially flourishing bacterial populations can corrupt their environment and thus cause their own extinction. The pH change resembles a 'public bad' that is collectively produced and harms all members of the population. This phenomenology can be recapitulated by a simple mathematical description based on negative feedback between the bacteria and the environmental pH (Supplementary Discussion and Supplementary Fig. 10).

Because the bacteria collectively change the pH, higher bacterial densities can deteriorate the environment more strongly and thus expedite ecological suicide. We tested this idea experimentally by measuring the fold growth within 24 h for different initial bacterial densities and different buffer concentrations. At low buffer concentrations, the bacteria die by ecological suicide independent of their initial density, whereas at high buffer concentrations they always survive (Fig. 2a). At intermediate buffer concentrations, however, survival becomes density dependent (Fig. 2a). For high initial cell densities, the bacteria die within 24 h, but below a critical initial density, the bacteria grow and survive. The fitness of the bacteria thus decreases markedly with increasing cell density. This aspect of ecological suicide is thus opposite to the well-known Allee effect, in which fitness increases with population density[18–20]. Although the observed death at high cell densities is reminiscent to death at high densities in common logistic growth models, in our experiments death continues until all cells have died out, whereas in logistic growth the density stabilizes at the carrying capacity.

What does this growth behaviour mean for the long-term growth dynamics of population such as those that occur during growth in medium with daily dilution into fresh medium? Figure 2a shows

[1]Physics of Living Systems, Department of Physics, Massachusetts Institute of Technology, Cambridge, MA, USA. [2]Arnold-Sommerfeld-Center for Theoretical Physics and Center for NanoScience, Ludwig-Maximilians-Universität München, Munich, Germany. [3]These authors contributed equally: Christoph Ratzke and Jonas Denk. *e-mail: cratzke@mit.edu; gore@mit.edu

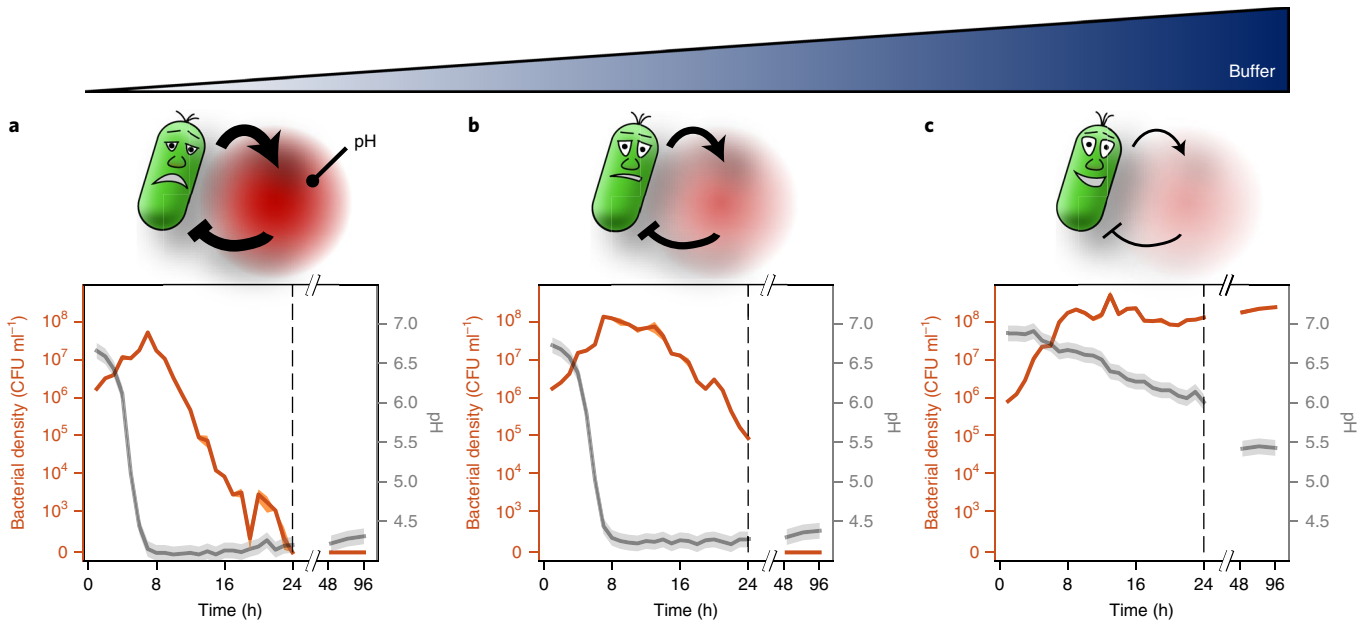

Fig. 1 | Microbial acidification can cause ecological suicide. *Paenibacillus* sp. were grown in a well-mixed batch culture in media containing 1% glucose as the main carbon source and minor amounts of complex nutrients (see Methods). **a**, At low buffer concentrations (10 mM phosphate, added as sodium dihydrogen phosphate), initially growing bacteria change the pH of the medium so markedly that they cause their own extinction. **b**,**c**, Adding increasing amounts of buffer (14 and 100 mM phosphate) tempers the acidification, and finally enables the survival of the bacteria. Mean bacterial density (CFU ml^{-1}) and s.e.m. are shown for three technical replicates in orange (solid line and shaded region, respectively). pH is shown in grey (solid line); the shaded region depicts the estimated measurement accuracy. The black vertical dashed lines show the 24 h mark.

how the bacterial density after one day of growth depends on the initial bacterial density. With intermediate buffering, the bacteria die for high initial densities but grow for low initial densities. This may cause oscillatory dynamics, since high bacterial densities cause low densities on the next day and vice versa. Indeed, this intuitive prediction is fully supported by a mathematical description based on negative feedback of the bacteria and the environmental pH alone, which shows a bifurcation of the end-of-the-day bacterial densities upon changing the buffer concentration (see Supplementary Information and Supplementary Figs. 11 and 12). To test this prediction, we cultured the bacteria in batch culture with a daily 1:100 dilution of the culture into fresh medium. As expected from Fig. 2a, with low buffering the bacteria go extinct on the first day and with high buffering they grow up to the same saturated density each day (Fig. 2c,e, Supplementary Figs. 6 and 8a). With intermediate buffering, however, the bacteria show oscillatory dynamics as predicted by our mathematical model (Fig. 2d, Supplementary Figs. 8b and 10). The oscillations in the population densities are accompanied by oscillations in the time at which the pH drops each day (acidification time, Fig. 2d and Supplementary Figs. 5 and 8b), which again shows the connection between pH change and ecological suicide. Ecological suicide caused by environmental deterioration therefore can drive oscillatory dynamics even in populations that consist of only one species.

We have seen that low bacterial densities lead to less deterioration of the environment and thus a less deadly effect on the bacteria. Therefore, effects that hinder bacterial growth by harming the bacteria may be able to save the population from ecological suicide. A first indication in this direction was found when changing the glucose concentration. Although one would expect that an increase in glucose concentrations is beneficial, in the presence of ecological suicide, the opposite is the case (Fig. 3a). At low glucose concentrations, the bacteria grow to lower densities, which hardly changes the pH and therefore allows the bacteria to survive. At high glucose concentrations, bacterial growth causes environmental acidification and thus ecological suicide. The bacterial population is therefore only able to survive in nutrient-poor conditions. Moreover, Figure 3a shows that ecological suicide can be observed even at rather low nutrient concentrations of around 0.2% glucose.

To explore the idea that environments that are usually considered poor can instead save the bacterial population, we measured the growth and survival of bacteria grown in the presence of the antibiotic kanamycin, or in the presence of ethanol or salt. Although these substances are different, they all inhibit bacterial growth and lead to similar profiles of population survival as a function of the concentration of the inhibiting substance (Fig. 3b–d). In the absence of harmful substances, the bacteria lower the pH to the point of extinction. At high concentrations, the harmful substances kill the bacteria. However, at intermediate concentrations, the bacteria can grow and survive. This leads to the paradoxical situation that substances that are normally used to kill bacteria in medicine (antibiotics) or food preservation (salt, ethanol) are able to save bacteria and enable their growth. The interplay between the harming substance and the ecological suicide results in a U-shaped dose–response curve of the harming substance, which is called hormesis in toxicology[21].

The effect of ecological suicide is surprising and has paradoxical consequences. However, the question arises: how common is ecological suicide in bacteria? To investigate this question, we incubated 119 bacterial soil isolates[22] from a broader taxonomic range (Supplementary Fig. 9) in the presence of glucose as a carbon source and urea as a nitrogen source. Glucose can be converted to organic acids and this acidifies the medium[23], whereas urea can be converted by many bacteria into ammonia and this alkalizes the environment[24]. From these 119 strains, the 21 strongest pH modifiers (either in acidic or alkaline directions) were tested for the presence of ecological suicide by measuring the fold growth in 24 h at low and high buffer concentrations (Fig. 4a). Indeed, around 25% of the strains suffered ecological suicide and were unable to survive at low buffer concentrations yet could be saved by more buffering (Fig. 4b). Another 20% grew better at high than low buffering, suggesting a

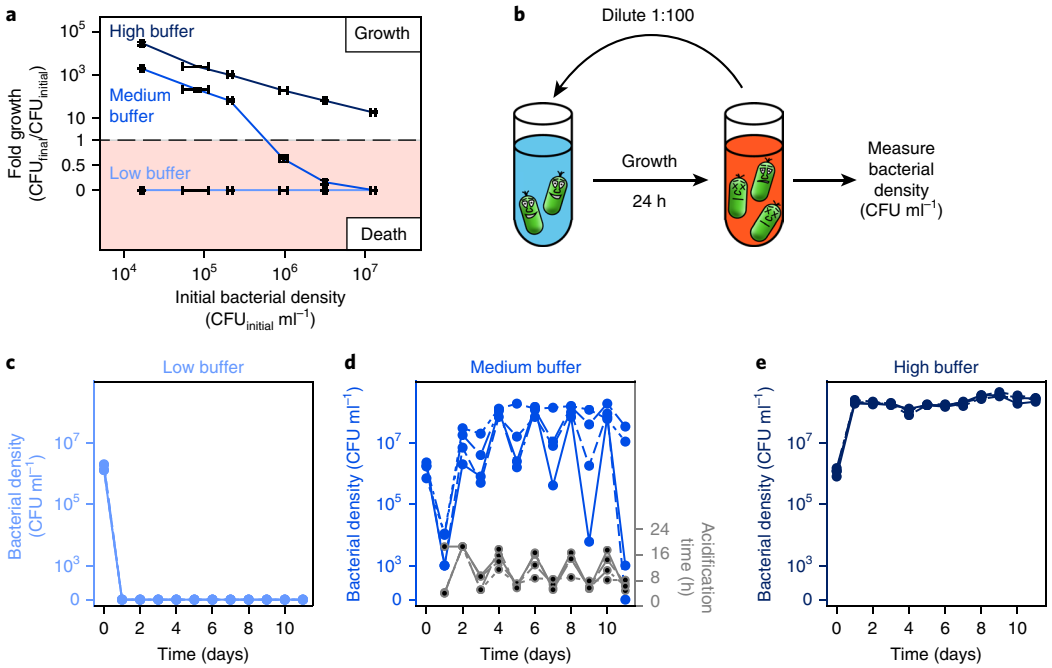

Fig. 2 | Ecological suicide can cause oscillations in the population size over time. a, At a low buffer concentration (10 mM phosphate), the bacteria commit ecologic suicide, whereas at a high buffer concentration (100 mM phosphate), the bacteria grow, in both cases independent of their initial density. However, at a moderate buffer concentration (26 mM phosphate), the bacteria die at high starting densities and grow at low starting densities. The fold growth at a high buffer concentration decreases for increasing initial bacterial densities, since the final bacterial density equals the carrying capacity and is therefore constant. Mean (solid lines) and s.e.m. (error bars) are shown for four replicates. The black horizontal dashed line corresponds to a fold growth of 1. **b**, To explore long time growth dynamics, the bacteria were grown in a daily dilution scheme with 24 h of incubation in well-mixed conditions followed by a 1:100 dilution into fresh medium. **c**,**e**, At low (10 mM phosphate; **c**) and high (100 mM phosphate; **e**) buffer conditions, the bacteria either die on the first day or grow to saturation every day. **d**, However, at medium buffer conditions, we measure oscillatory dynamics of the bacterial density. This is accompanied by oscillations in the time that the bacteria need to acidify the environment (acidification time, Supplementary Fig. 8). The exact type of oscillatory dynamics depends on the slope and shape of the curve in **a**, as discussed in more detail in the Supplementary Information. **c**–**e**, The four blue lines (solid, dashed, dotted, dashed-dotted; the separated curves can be seen in Supplementary Fig. 5) show different replicates. The strong differences between the replicates highlight the sensitivity of these oscillations to experimental conditions and that they probably do not show a limit cycle oscillation.

self-inhibiting but non-deadly effect of the pH. Finally, one species even changed the pH in ways that supported its own growth (an effect discussed in more detail elsewhere[9]). These results show that ecological suicide is not an exotic effect but appears rather often and its occurrence in nature should be investigated further in the future.

Discussion

We demonstrated that microbes are able to cause their own extinction by deteriorating the environment, a process that we call ecological suicide. Several cases are described in which microbial populations experience a slow decline after reaching saturation[25,26]. However, this decline is usually very slow compared to the growth rate and does not cause sudden population extinction. In ecological suicide, however, the population does not even reach saturation; instead, the bacteria switch immediately from a growth into a death phase (Fig. 1a). A notable exception are quorum sensing deficient mutants of several *Burkholderia* species that show a type of ecological suicide[27], whereas in the wild-type strains quorum sensing mediates a change in metabolism that avoids ecological suicide. This shows that bacteria can possess mechanisms that actively counteract ecological suicide[27–29].

A phenomenon similar but not identical to ecological suicide is population overshoot, which is often connected to overexploitation of natural resources and has been proposed in several macro-organisms[30–32], but it is mostly discussed in humans that overexploit the environment[33–35]. Several ancient civilizations are suspected to have collapsed by overexploitation of natural resources[36–38]. Upon overshoot, a population exceeds the long-term carrying capacity of its ecosystem, followed by a drop of the population below the carrying capacity, which usually does not lead to extinction of the population but is followed by recovery at a lower density[30,35]. However, in our case of ecological suicide, the carrying capacity of the ecosystem is changed to zero—the bacteria produce a deadly environment and go extinct without recovery, which marks ecological suicide as an extreme version of population overshoot.

With daily dilutions, ecological suicide can result in oscillatory behaviour. Oscillations in ecology have been intensely studied, often as a consequence of species interactions[39,40]; in our system the second species is replaced by the pH value, resulting in a situation in which interactions between one species and its environment drive the oscillations. In a similar way, modification of and reacting to the environment have recently been described to cause metabolic oscillations in yeast[41], expanding waves in microbial biofilms[42] or oscillations in populations densities by toxin production or resource competition[43,44].

In view of the high frequency of ecological suicide that we observed in natural isolates of soil bacteria, this effect may have a broad impact on microbial ecosystems in terms of microbial interactions and biodiversity[9] and its occurrence and ecological meaning in nature have to be investigated in the future. Moreover, ecological suicide can happen on different carbon sources, at a lower temperature of 22 °C—although sufficiently low temperatures may stop ecological suicide—and even with complex sugars and thus under conditions that more resemble those in the soil (Supplementary Fig. 1). In our case, the ecological suicide was mediated by the pH, but changing any environmental parameter, such as oxygen levels

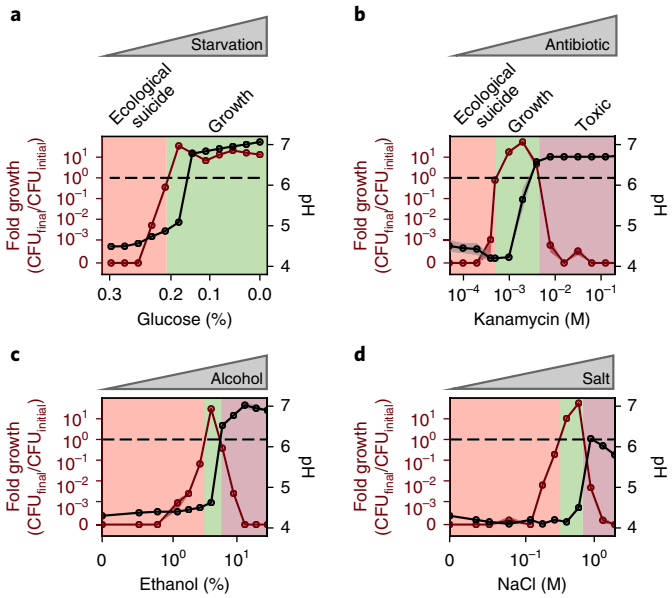

Fig. 3 | Inhibiting growth of the bacteria can save the population. **a**, Reducing sugar concentration prevents ecological suicide. **b**–**d**, At moderate concentrations, the addition of bactericidal substances, such as antibiotics (**b**) or alcohol (**c**), or high amounts of sodium chloride (**d**) can save the population from ecological suicide. Open circles and shaded regions depict, respectively, the mean and s.e.m. of four replicates (red, fold growth; black, pH). All values are final values after 24 h. The black horizontal dashed lines correspond to a fold growth of 1.

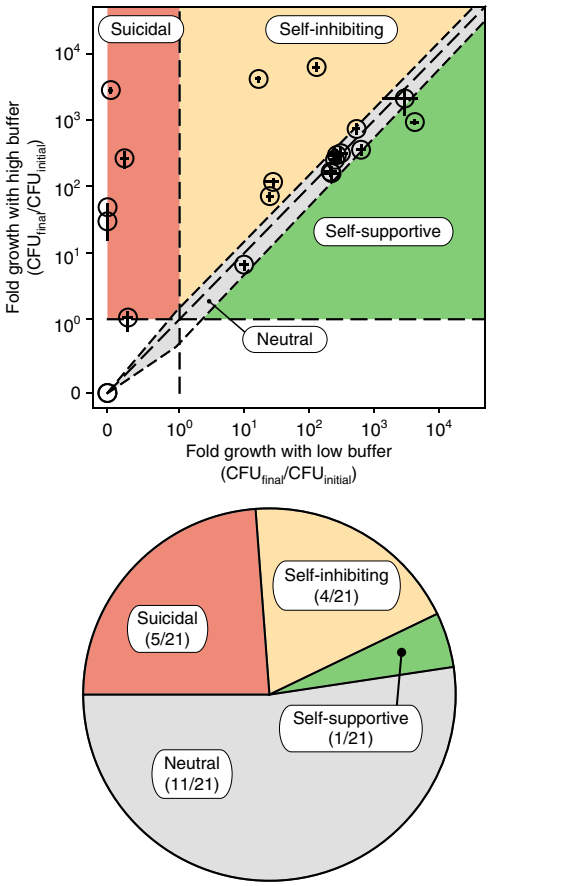

Fig. 4 | Ecological suicide is a common phenomenon in microbes. Twenty-one bacteria that strongly modified the pH were tested for ecological suicide by growing them on a medium containing 1% glucose and 0.8% urea at low buffer (10 mM phosphate) and high buffer (100 mM phosphate) conditions. Bacteria that die at low buffer but grow at high buffer concentrations were counted as ecological suicide (suicidal, 5 bacterial species). Bacteria that grow slower at low buffer than high buffer conditions are called self-inhibiting (4 bacterial species). Bacteria that grow in similar ways at low and high buffer (growth in one buffer condition is between equal and 1.5-fold relative to growth in the other condition) were called neutral (11 bacterial species) and bacteria that grow better with low than with high buffer are called self-supportive (1 species). The circles mark the mean of eight replicates for each individual bacterial species. The lengths of the bars denote the s.e.m. in *x* and *y* direction.

or metabolite concentrations in self-harming ways may cause similar outcomes.

Our findings raise the question of how such self-inflicted death of microbes can exist without evolution selecting against them. We hypothesize that, although ecological suicide is detrimental for the population, it may be evolutionary beneficial for the individual bacterium. A fast metabolism of glucose may harm and even kill the population but benefits the individual compared to an individual that takes the burden of slower glucose metabolism to save the population. The phenomena of ecological suicide could therefore be an end-product of evolutionary suicide[45]. Future work should explore the evolutionary origin of ecological suicide as well as the consequences of this phenomenon for the ecology and evolution of microbes.

Methods

All chemicals were purchased from Sigma-Aldrich (St Louis, USA), if not stated otherwise.

Buffer. For precultures of the bacteria the basic buffer recipe was 10 g l^{-1} yeast extract and 10 g l^{-1} soytone (both Becton Dickinson, Franklin Lakes, USA). We refer to this buffer as 1× nutrient medium (also 1×Nu). The initial pH of this medium was 7 and 100 mM phosphate was added. For the washing steps and the experiments itself the medium contained 1 g l^{-1} yeast extract and 1 g l^{-1} soytone, 0.1 mM $CaCl_2$, 2 mM $MgCl_2$, 4 mg l^{-1} $NiSO_4$, 50 mg l^{-1} $MnCl_2$ and 1× Trace Element Mix (Teknova, Hollister, USA). We refer to this buffer as the base buffer. It was supplemented with phosphate buffer and/or glucose as outlined in the different experiments. The usual concentration was 10 g l^{-1} glucose, deviations from this concentration are described for the different experiments below. All media were filter-sterilized.

Estimation of CFU. To estimate the number of living bacteria in the different experiments we used colony counting. At the end of every growth cycle, a dilution row of the bacteria was made by diluting them once 1:100 and six times 1:10 in phosphate-buffered saline (PBS; Corning, New York, USA). With a 96-well pipette (Viaflo 96, Integra Biosciences, Hudson, USA) 10 µl of every well for every dilution step was transferred to an agar plate (Tryptic Soy Broth (Teknova, Hollister, USA), 2.5% agar (Becton Dickinson, Franklin Lakes, USA) with a 150-mm diameter. The droplets were allowed to dry and the plates were incubated at 30 °C for 1–2 days until clear colonies were visible. The different dilution steps ensured that a dilution could be found that enabled the counting of colonies.

pH measurements. To measure the pH directly in the bacterial growth culture at the end of each growth cycle, a pH microelectrode (N6000BNC, SI Analytics, Weilheim, Germany) was used. The grown bacterial cultures were transferred into 96-well PCR plates (VWR, Radnor, USA) that enabled the measurement of pH values in less than 200 µl.

Bacterial culture. All cultures were incubated at 30 °C. The precultures were carried out in 5 ml medium in 50 ml culture tubes (Falcon, Becton Dickinson, Franklin Lakes, USA) overnight in 1× Nu with an additional 100 mM phosphate. The shaking speed was 250 r.p.m. on a New Brunswick Innova 2100 shaker (Eppendorf, Hauppauge, USA), the lids of the Falcon tubes were only slightly screwed on to enable gas exchange. Except for the 24 h experiment with hourly measurements, which were done in 50 ml culture tubes (Falcon, Becton Dickinson, Franklin Lakes, USA), the experiments were all done in 500-µl 96-deepwell plates (Deepwell Plate 96/500 µl, Eppendorf, Hauppauge, USA) covered with two sterile AearaSeal adhesive sealing films (Excell Scientific, Victorville, USA), the plates were shaken at 1,350 r.p.m. on Heidolph platform shakers (Titramax 100, Heidolph North America, Elk Grove Village, USA). The culture volume was 200 µl if not

stated otherwise. To avoid evaporation the shakers were covered with a custom made polyacryl box (Wetinator 2000) with small water reservoirs placed within.

Preculture and preparation of bacteria. For these experiments *Paenibacillus* sp. was used, a bacterium that can acidify the environment but cannot tolerate low pH values. The bacteria were grown at 30 °C. The preculture of *Paenibacillus* sp. was done in 5 ml 1× Nu, pH 7 with 100 mM phosphate for around 14 h. *Paenibacillus* sp. was diluted 1:100 into the same medium and grown to an optical density (OD) cm^{-1} of 2. The bacterial solution was washed twice with base buffer with 10 mM phosphate, pH 7. The bacteria were resuspended in the same base buffer and the OD cm^{-1} was adjusted to 2. The buffer concentration of the base buffer was chosen as described in the experiments below.

24 h experiment with hourly measurement of cell density and pH. The 24 h experiment is shown in Fig. 1. Tubes were prepared by adding 10 ml base with 10 $g\,l^{-1}$ glucose and different phosphate concentrations of 10, 14 and 100 mM. The bacteria were added by 1:100 dilution. The tubes were incubated at 30 °C, 1,350 r.p.m. shaking. Every hour, 200 µl was taken from each tube, the CFU was estimated and the pH measured. For every measurement three technical replicates were carried out.

Density dependence of growth. Density-dependence experiments are shown in Fig. 2a. The 96-deepwell plates were prepared by adding 200 µl base buffer containing 10 $g\,l^{-1}$ glucose and different phosphate concentrations ranging from 10 to 100 mM (see main text). To obtain different initial densities of bacteria, the bacteria were added by different dilutions ranging from 1:10 to $(1/4)^5$:10 dilution. The 96-deepwell plates were incubated at 30 °C, 1,350 r.p.m. shaking. At the beginning of the experiment as well as after 24 h, the CFU was estimated. After 24 h, the pH was measured. For every condition there were two biological replicates and two technical replicates.

Growth under daily dilution. Daily dilution experiments are shown in Fig. 2b–d. The 96-deepwell plates were prepared as for the 'density dependence of growth' experiment. The bacteria were added by 1:100 dilution. The 96-deepwell plates were incubated at 30 °C, 1,350 r.p.m. shaking. At the beginning of the experiment as well as after 24 h, the CFU was estimated. After 24 h, the pH was measured. Every 24 h, the CFU was estimated, the pH was measured and the bacteria were diluted 1:100 into fresh medium. To study the dynamics of bacterial growth and the pH, at the beginning of each day, the bacteria were also diluted 1:100 into a 96-well plate (96 Well Clear Flat Bottom Tissue Culture-Treated Culture Microplate, 353072, Falcon, Corning, USA) with the same medium in each well as for the 500-µl 96-deepwell plate. In addition, every well was supplemented by fluorescent nanobeads (1:100 dilution), which we fabricated as described below. In parallel to the incubation of the 500-µl 96-deepwell plate, this 96-well plate was then analysed in a Tecan infinite 200 Pro (Tecan, Männedorf, Switzerland) at 30 °C, 182 r.p.m., 4 mm amplitude. For this experiment, the optical density was measured by absorbance and the fluorescence of the nanobeads was measured by exciting fluorescein (excitation wavelength 450 nm, emission wavelength 516 nm) and tetrakis(pentafluorophenyl) porphyrin (TFPP; excitation wavelength 582 nm, emission wavelength 658 nm). Measuring the optical density of the bacteria and the fluorescence of the nanobeads every 15 min over the course of one day, enabled us to track the change in pH. Although the optical density and fluorescence were measured in parallel growing 96-well plates, we argue that they (at least qualitatively) capture the dynamics in the 96-deepwell plate, which is underlined by the fact that the measured acidification time and bacterial density oscillate synchronous (Fig. 2d). Parallel to the oscillations in the CFU observed in the 96-deepwell plates, the fluorescence measurements in the 96-well plates display oscillations in the timepoint, the pH drops, that is, the timepoints of the fluorescence intensity's turning points (see Fig. 2d, Supplementary Fig. 2). For every buffer condition there were four biological replicates in the 96-well and 96-deepwell plates.

Fabrication of fluorescent nanobeads. To study the change in pH during our daily dilution experiments, we fabricated fluorescent nanobeads following a previously established protocol[46]. These nanobeads contain fluorescein, for which the fluorescence intensity depends on the pH[47], and a highly photostable fluorinated porphyrin (TFPP), which acts as a red-emitting reference dye. Because the fluorescence intensity of TFPP is independent of pH, it serves as internal standard to make the result independent of the overall nanobead concentration. Thus the ratio of the fluorescein and TFPP fluorescence signals is a function only of the pH value (Supplementary Fig. 4).

Effect of harmful conditions on bacterial survival. Survival experiments are shown in Fig. 3. The preculture was done overnight in 1× Nu, pH 7 with 100 mM phosphate. After 15 h, the bacteria were diluted 1:100 into the same medium. Upon reaching an OD cm^{-1} of 2, the bacteria were washed twice with base buffer and the OD cm^{-1} was adjusted to 2. The bacteria were diluted 1:100 into 96-deepwell plates (Eppendorf, Hauppauge, USA) containing base medium, pH 7 with 10 $g\,l^{-1}$ glucose and different amounts of kanamycin, NaCl or ethanol. For Fig. 3a, the glucose concentration was varied. The bacteria were incubated for 24 h at 30 °C, 1,350 r.p.m. on a Heidolph platform shakers (Titramax 100, Heidolph North America, Elkove Village, USA) as described above. The live cell density was estimated by colony counting at the start of the experiment and after 24 h. The pH was measured after 24 h with a pH microelectrode as described above.

Frequency of ecological suicide. For the experiment shown in Fig. 4, 21 different soil bacteria were used, which were identified out of 119 soil bacteria to yield the highest change in pH. The 119 bacterial strains were isolated from a single grain of soil collected in September 2015 in Cambridge, Massachusetts, USA. The grain weighed approximately 1 mg and was handled using sterile technique. The grain was washed in PBS and serial dilutions of the supernatant were plated on nutrient agar (0.3% yeast extract, 0.5% peptone, 1.5% bacto agar) and incubated for 48 h at room temperature. Isolated colonies were sampled and cultured at room temperature in 5 ml nutrient broth (0.3% yeast extract, 0.5% peptone) for 48 h. To ensure purity, the liquid cultures of the isolates were diluted in PBS and plated on nutrient agar. Single colonies picked from these plates were once again grown in nutrient broth for 48 h at room temperature and the resulting stocks were stored in 20% glycerol at −80 C. The 16S rRNA gene was sequenced using Sanger sequencing of DNA extracted from glycerol stocks carried out at GENEWIZ (South Plainfield, New Jersey, USA). Sequencing was performed in both directions using the company's universal 16S rRNA primers, yielding assembled sequences around 1,100 nt in usable length. Some of those strains have been in more detail investigated previously[24].

In order to identify the 21 species that caused the strongest pH change, precultures of the 119 soil bacteria were done in 200 µl 1× Nu, pH 7 with 100 mM phosphate for 14 h at room temperature, 800 r.p.m. shaking. The precultures were then diluted 1:100 into the same medium and grown for 6 h, which approximately corresponded to a growth to an OD cm^{-1} of 2 for the precultures of *Paenibacillus* sp. used in the *Paenibacillus* sp. experiments described above. The bacteria were then diluted 1:100 into fresh medium and grown for 24 h at room temperature, 800 r.p.m. shaking. After 24 h, the bacterial density (CFU ml^{-1}) and pH of all cultures were measured and the 21 bacteria with the highest change in pH were selected.

For these 21 species, precultures were done in 5 ml 1× Nu, pH 7 with 100 mM phosphate for 14 h. The cultures were diluted 1:100 into the same medium and grown to an OD cm^{-1} of approximately 2. The bacteria were resuspended in the same base medium and the OD cm^{-1} was adjusted to 2. To categorize the species according to 'suicidal', 'self-inhibiting', 'self-supporting' and 'neutral' each species was grown in the same base medium once with a high buffer concentration (100 mM phosphate) and once with a low buffer concentration (10 mM phosphate). At the start of the experiment and after 24 h, the CFU was estimated. The pH was measured after 24 h with a pH microelectrode as described above.

Reporting Summary. Further information on experimental design is available in the Nature Research Reporting Summary linked to this article.

Data availability. All data generated or analysed during this study are included in the Article (and its Supplementary Information).

Received: 30 August 2017; Accepted: 14 March 2018;
Published online: 16 April 2018

References

1. Celiker, H. & Gore, J. Cellular cooperation: insights from microbes. *Trends Cell Biol.* **23**, 9–15 (2013).
2. Ratzke, C. & Gore, J. Self-organized patchiness facilitates survival in a cooperatively growing *Bacillus subtilis* population. *Nat. Microbiol.* **1**, 16022 (2016).
3. Drescher, K., Nadell, C. D., Stone, H. A., Wingreen, N. S. & Bassler, B. L. Solutions to the public goods dilemma in bacterial biofilms. *Curr. Biol.* **24**, 50–55 (2014).
4. Celiker, H. & Gore, J. Competition between species can stabilize public-goods cooperation within a species. *Mol. Syst. Biol.* **8**, 621 (2012).
5. Anderson, D. E., Becktel, W. J. & Dahlquist, F. W. pH-induced denaturation of proteins: a single salt bridge contributes 3-5 kcal/mol to the free energy of folding of T4 lysozyme. *Biochemistry* **29**, 2403–2408 (1990).
6. Träuble, H., Teubner, M., Woolley, P. & Eibl, H. Electrostatic interactions at charged lipid membranes: I. Effects of ph and univalent cations on membrane structure. *Biophys. Chem.* **4**, 319–342 (1976).
7. Jones, R. T. et al. A comprehensive survey of soil acidobacterial diversity using pyrosequencing and clone library analyses. *ISME J.* **3**, 442–453 (2009).
8. Rousk, J., Brookes, P. C. & Bååth, E. Contrasting soil pH effects on fungal and bacterial growth suggest functional redundancy in carbon mineralization. *Appl. Environ. Microbiol.* **75**, 1589–1596 (2009).
9. Ratzke, C. & Gore, J. Modifying and reacting to the environmental pH can drive bacterial interactions. *PLoS Biol.* **16**, e2004248 (2018).

10. Russell, J. B. & Dombrowski, D. B. Effect of pH on the efficiency of growth by pure cultures of rumen bacteria in continuous culture. *Appl. Environ. Microbiol.* **39**, 604–610 (1980).
11. Raven, J. A. & Smith, F. A. The evolution of chemiosmotic energy coupling. *J. Theor. Biol.* **57**, 301–312 (1976).
12. Safařík, I. V. O. & Šantrůčková, H. Direct determination of total soil carbohydrate content. *Plant Soil* **143**, 109–114 (1992).
13. Mehta, N. C., Dubach, P. & Deuel, H. in *Advances in Carbohydrate Chemistry* (ed. Wolfrom, M. L.) 335–355 (Academic, Amsterdam, 1962).
14. Li, C. H., Ma, B. L. & Zhang, T. Q. Soil bulk density effects on soil microbial populations and enzyme activities during the growth of maize (*Zea mays* L.) planted in large pots under field exposure. *Can. J. Soil Sci.* **82**, 147–154 (2002).
15. Raynaud, X. & Nunan, N. Spatial ecology of bacteria at the microscale in soil. *PLoS ONE* **9**, e87217 (2014).
16. Seviour, R. & Nielsen, P. H. *Microbial Ecology of Activated Sludge* (IWA Publishing, London, 2010).
17. Seviour, E. M. et al. Studies on filamentous bacteria from Australian activated sludge plants. *Water Res.* **28**, 2335–2342 (1994).
18. Allee, W. C. et al. *Principles of Animal Ecology* (W. B. Saunders, Philadelphia, 1965).
19. Courchamp, F., Clutton-Brock, T. & Grenfell, B. Inverse density dependence and the Allee effect. *Trends Ecol. Evol.* **14**, 405–410 (1999).
20. Stephens, P. A., Sutherland, W. J. & Freckleton, R. P. What is the Allee effect? *Oikos* **87**, 185–190 (1999).
21. Stebbing, A. R. D. Hormesis — the stimulation of growth by low levels of inhibitors. *Sci. Total Environ.* **22**, 213–234 (1982).
22. Higgins, L. M., Friedman, J., Shen, H. & Gore, J. Co-occurring soil bacteria exhibit a robust competitive hierarchy and lack of non-transitive interactions. Preprint at https://www.biorxiv.org/content/early/2017/08/16/175737 (2017).
23. Paczia, N. et al. Extensive exometabolome analysis reveals extended overflow metabolism in various microorganisms. *Microb. Cell Factor.* **11**, 122 (2012).
24. Fujita, Y., Ferris, F. G., Lawson, R. D., Colwell, F. S. & Smith, R. W. Subscribed content calcium carbonate precipitation by ureolytic subsurface bacteria. *Geomicrobiol. J.* **17**, 305–318 (2000).
25. Finkel, S. E. Long-term survival during stationary phase: evolution and the GASP phenotype. *Nat. Rev. Microbiol.* **4**, 113–120 (2006).
26. Burtner, C. R., Murakami, C. J., Kennedy, B. K. & Kaeberlein, M. A molecular mechanism of chronological aging in yeast. *Cell Cycle* **8**, 1256–1270 (2009).
27. Goo, E. et al. Bacterial quorum sensing, cooperativity, and anticipation of stationary-phase stress. *Proc. Natl Acad. Sci. USA* **109**, 19775–19780 (2012).
28. An, J. H., Goo, E., Kim, H., Seo, Y.-S. & Hwang, I. Bacterial quorum sensing and metabolic slowing in a cooperative population. *Proc. Natl Acad. Sci. USA* **111**, 14912–14917 (2014).
29. Cotter, P. D. & Hill, C. Surviving the acid test: responses of gram-positive bacteria to low pH. *Microbiol. Mol. Biol. Rev.* **67**, 429–453 (2003).
30. Klein, D. R. The introduction, increase, and crash of reindeer on St. Matthew Island. *J. Wildl. Manage.* **32**, 350–367 (1968).
31. Scheffer, V. B. The rise and fall of a reindeer herd. *Sci. Mon.* **73**, 356–362 (1951).
32. Hindell, M. A. Some life-history parameters of a declining population of southern elephant seals, *Mirounga leonina*. *J. Anim. Ecol.* **60**, 119–134 (1991).
33. Wackernagel, M. et al. Tracking the ecological overshoot of the human economy. *Proc. Natl Acad. Sci. USA* **99**, 9266–9271 (2002).
34. Malthus, T. R. *An Essay on the Principle of Population, as it Affects the Future Improvement of Society: With Remarks on the Speculations of Mr. Godwin, Mr. Condorcet, and Other Writers* (J. Johnson, London, 1798).
35. Meadows, D., Randers, J. & Meadows, D. *Limits to Growth: The 30-Year Update* (Chelsea Green Publishing, White River Junction, 2004).
36. Diamond, J. *Collapse: How Societies Choose to Fail or Succeed* (Penguin, London, 2005).
37. Tainter, J. A. Archaeology of overshoot and collapse. *Annu. Rev. Anthropol.* **35**, 59–74 (2006).
38. Shennan, S. et al. Regional population collapse followed initial agriculture booms in mid-Holocene Europe. *Nat. Commun.* **4**, 2486 (2013).
39. Fussmann, G. F., Ellner, S. P., Shertzer, K. W. & Hairston, N. G. Jr. Crossing the Hopf bifurcation in a live predator–prey system. *Science* **290**, 1358–1360 (2000).
40. Yurtsev, E. A., Conwill, A. & Gore, J. Oscillatory dynamics in a bacterial cross-protection mutualism. *Proc. Natl Acad. Sci. USA* **113**, 6236–6241 (2016).
41. Tu, B. P., Kudlicki, A., Rowicka, M. & McKnight, S. L. Logic of the yeast metabolic cycle: temporal compartmentalization of cellular processes. *Science* **310**, 1152–1158 (2005).
42. Liu, J. et al. Coupling between distant biofilms and emergence of nutrient time-sharing. *Science* **365**, 638–642 (2017).
43. Collos, Y. et al. Phased oscillations in cell numbers and nitrate in batch cultures of *Alexandrium tamarense* (Dinophyceae). *J. Phycol.* **47**, 1057–1062 (2011).
44. Cornejo, O. E., Rozen, D. E., May, R. M. & Levin, B. R. Oscillations in continuous culture populations of *Streptococcus pneumoniae*: population dynamics and the evolution of clonal suicide. *Proc. R. Soc. B* **276**, 999–1008 (2009).
45. Parvinen, K. Evolutionary suicide. *Acta Biotheor.* **53**, 241–264 (2005).
46. Wang, X., Meier, R. J. & Wolfbeis, O. S. Fluorescent pH-sensitive nanoparticles in an agarose matrix for imaging of bacterial growth and metabolism. *Angew. Chem. Int. Ed.* **52**, 406–409 (2013).
47. Rein, J. et al. Fluorescence measurements of serotonin-induced V-ATPase-dependent pH changes at the luminal surface in salivary glands of the blowfly *Calliphora vicina*. *J. Exp. Biol.* **209**, 1716–1724 (2006).

Acknowledgements

We thank L. Higgins for providing us with the collection of bacterial soil isolates. J.D. is supported by a DFG fellowship through the Graduate School of Quantitative Biosciences Munich. We thank all members of the Gore lab for reading and discussing the manuscript. This work was funded by an Allen Distinguished Investigator Award and a NIH R01 grant.

Author contributions

C.R., J.D. and J.G. designed the research. J.D., C.R. and J.G. carried out the experiments and performed the mathematical analysis. C.R., J.D. and J.G discussed and interpreted the results, and wrote the manuscript.

Competing interests

The authors declare no competing interests.

Additional information

Supplementary information is available for this paper at https://doi.org/10.1038/s41559-018-0535-1.

Reprints and permissions information is available at www.nature.com/reprints.

Correspondence and requests for materials should be addressed to C.R. or J.G.

Publisher's note: Springer Nature remains neutral with regard to jurisdictional claims in published maps and institutional affiliations.

nature research

Corresponding author(s): Christoph Ratzke, Jeff Gore

☐ Initial submission ☐ Revised version ☒ Final submission

Life Sciences Reporting Summary

Nature Research wishes to improve the reproducibility of the work that we publish. This form is intended for publication with all accepted life science papers and provides structure for consistency and transparency in reporting. Every life science submission will use this form; some list items might not apply to an individual manuscript, but all fields must be completed for clarity.

For further information on the points included in this form, see Reporting Life Sciences Research. For further information on Nature Research policies, including our data availability policy, see Authors & Referees and the Editorial Policy Checklist.

Experimental design

1. Sample size

Describe how sample size was determined.

The experiments turned out to be very reproducible, thus the error between different replicas and thus the error bars are very small. Moreover, are results and conclusions are not based statastic methods but are of rather qualitative nature. Because of these reasons we found at least 3 replicates for each quantitative measurement sufficient.

2. Data exclusions

Describe any data exclusions.

We excluded the data of one replica in Supplemental Fig. 3. This data curve showed a very strong optical density at time=0 and strong fluctuations of the signal over time, which we assigned to the presence of contaminations from the beginning of the measurement on (e.g aggregated nanobeads or similar) and removed that curve.

3. Replication

Describe whether the experimental findings were reliably reproduced.

We reproduces every measurement at least 2 times, by two independent people (J.D and C.R.) with the same results. Often measurements were reproduced also more often than 2 times.

4. Randomization

Describe how samples/organisms/participants were allocated into experimental groups.

There was no randomization.

5. Blinding

Describe whether the investigators were blinded to group allocation during data collection and/or analysis.

We did not use blinding. The signals and the differences between the different measurements were very clear, which did not make blinding necessary.

Note: all studies involving animals and/or human research participants must disclose whether blinding and randomization were used.

6. Statistical parameters

For all figures and tables that use statistical methods, confirm that the following items are present in relevant figure legends (or in the Methods section if additional space is needed).

n/a	Confirmed
☐	☒ The exact sample size (*n*) for each experimental group/condition, given as a discrete number and unit of measurement (animals, litters, cultures, etc.)
☐	☒ A description of how samples were collected, noting whether measurements were taken from distinct samples or whether the same sample was measured repeatedly
☐	☒ A statement indicating how many times each experiment was replicated
☒	☐ The statistical test(s) used and whether they are one- or two-sided (note: only common tests should be described solely by name; more complex techniques should be described in the Methods section)
☒	☐ A description of any assumptions or corrections, such as an adjustment for multiple comparisons
☒	☐ The test results (e.g. *P* values) given as exact values whenever possible and with confidence intervals noted
☒	☐ A clear description of statistics including central tendency (e.g. median, mean) and variation (e.g. standard deviation, interquartile range)
☐	☒ Clearly defined error bars

See the web collection on statistics for biologists for further resources and guidance.

Software

Policy information about availability of computer code

7. Software

Describe the software used to analyze the data in this study.	to solve the differential equations we used NDSolve[] in Wolfram Mathematica 11

For manuscripts utilizing custom algorithms or software that are central to the paper but not yet described in the published literature, software must be made available to editors and reviewers upon request. We strongly encourage code deposition in a community repository (e.g. GitHub). *Nature Methods* guidance for providing algorithms and software for publication provides further information on this topic.

Materials and reagents

Policy information about availability of materials

8. Materials availability

Indicate whether there are restrictions on availability of unique materials or if these materials are only available for distribution by a for-profit company.	The soil strains we used are avaiable on request, other than that no unique material has been used.

9. Antibodies

Describe the antibodies used and how they were validated for use in the system under study (i.e. assay and species).	No antibodies were used.

10. Eukaryotic cell lines

a. State the source of each eukaryotic cell line used.	No eukaryotic cell lines were used.
b. Describe the method of cell line authentication used.	No eukaryotic cell lines were used.
c. Report whether the cell lines were tested for mycoplasma contamination.	No eukaryotic cell lines were used.
d. If any of the cell lines used are listed in the database of commonly misidentified cell lines maintained by ICLAC, provide a scientific rationale for their use.	No eukaryotic cell lines were used.

Animals and human research participants

Policy information about studies involving animals; when reporting animal research, follow the ARRIVE guidelines

11. Description of research animals

Provide details on animals and/or animal-derived materials used in the study.	No animals were used.

Policy information about studies involving human research participants

12. Description of human research participants

Describe the covariate-relevant population characteristics of the human research participants.	No humans were used.

Supplementary Materials for

Ecological suicide in microbes

Christoph Ratzke*[1†], Jonas Denk*[2] and Jeff Gore[1†]

[1] **Physics of Living Systems, Department of Physics, Massachusetts Institute of Technology, Cambridge, MA, USA**

[2] **Arnold-Sommerfeld-Center for Theoretical Physics and Center for NanoScience, Ludwig-Maximilians-Universität München, Theresienstraße 37, D-80333 München, Germany**

*equal contribution

[†] correspondence should be sent to: cratzke@mit.edu or gore@mit.edu

Supplementary Text

In these Supplementary Notes we further elaborate our dynamical analysis of ecological suicide in microbes. We first discuss the dependence of the fluorescence intensity of our fabricated nanobeads (see Methods) on the pH. Then, we present time resolved measurements of the optical density and the fluorescence intensity of these nanobeads throughout our daily dilution experiments.

To test our conceptual understanding of ecological suicide in *Paenibacillus sp.* (Ps), we present a mathematical description based on our experimental observations. We show that the proposed mathematical equations capture the complete phenomenology of ecological suicide in Ps, including non-monotonic growth dynamics and oscillatory behavior in daily dilutions.

Paenibacillus sp. isolation and phylogeny:

The *Paenibacillus sp.* was isolated from a grain of soil collected in Cambridge, MA, USA and was part of a soil species collection that will be described in more detail elsewhere (Logan Higgins et al, in prep). The 16S rRNA of this strain was sequenced and is most closely related to *Paenibacillus tundrae A10b* [1] according to RDB/SeqMatch tool [2] with a similarity score of 0.995 and a S_ab score of 0.975. For a characterization of all 21 species shown in Fig.4, please refer to Fig. S9. Also here we used the to RDB/SeqMatch tool and assigned the used bacteria to their closest related bacteria based in the maximal similarity score and S_ab.. For a characterization of all 21 species shown in Fig.4, please refer to Supplementary Fig. 9. Also here we used the to RDB/SeqMatch tool and assigned the used bacteria to their closest related bacteria based in the maximal similarity score and S_ab.

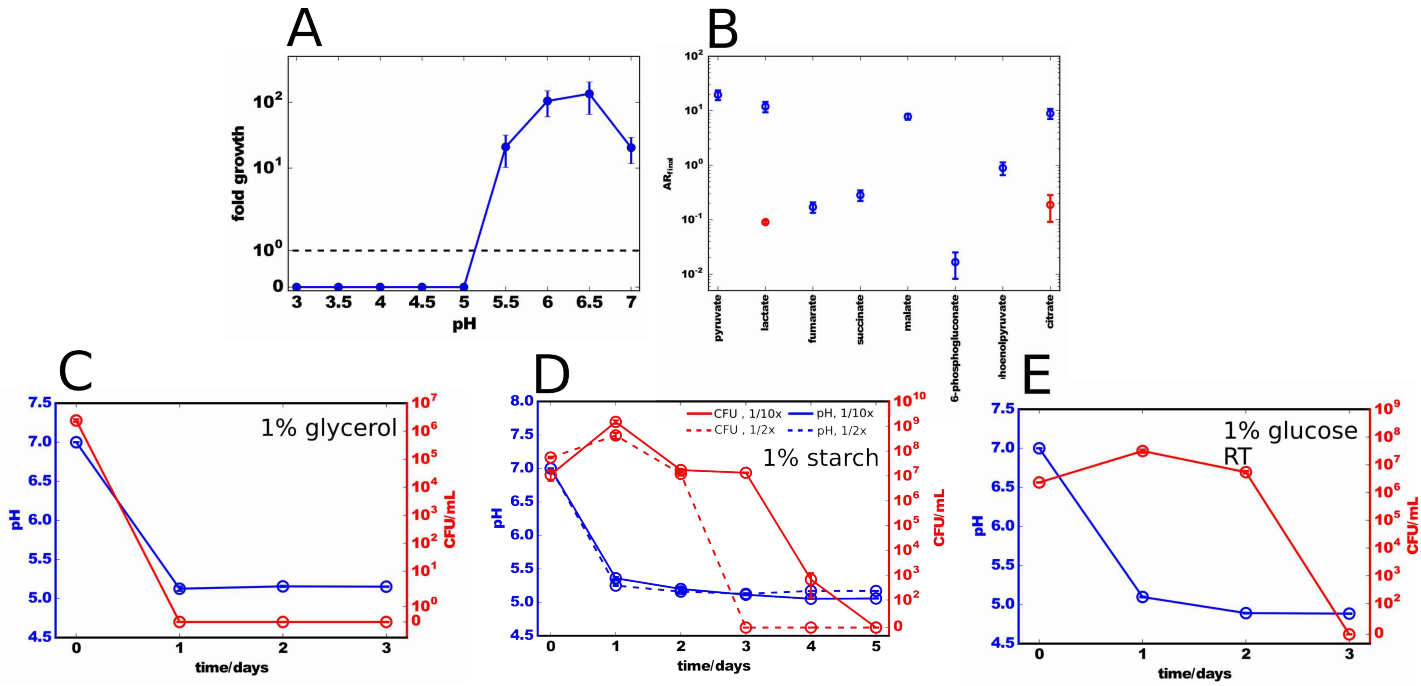

Supplementary Fig. 1: Growth of Paenibacillus sp. at different pH values, secretion of organic acids and ecological suicide under different conditions. *(A) The CFU were measured at the beginning and end of 24 hours of growth. The fold growth is the ratio of final/initial CFU. At low pH values the bacteria die. The horizontal dashed line marks a fold growth of 1 - eg the cell number did not change over 24 hours. The errorbars are SEM from three replicates. (B) Paenibacillus sp. was grown in M9 media with 2% glucose as the only carbon source. Mass spectrometry of the supernatant indicated that a variety of organic acids were produced by the bacteria. Pyruvate and lactate could be detected in the original media (red circles) but increased in concentration upon bacterial growth. Several other organic acids could not be detected in the original media but accumulated upon bacterial growth. Organic acid secretion can possibly be a result of a type of overflow metabolism*[9]*. AR is the area ratio of the area under the curve for the detected substance divided by the area under the curve of an internal standard (isotope labeled amino acid). Ecological suicide is observed on 1% glycerol (C), on the complex carbohydrate starch (D), and at room temperature, ~22°C (E). For (C) and (E) the experiment was performed similar to the experiments probing the ecological suicide on glucose and as described in the Methods, but with glycerol or at room temperature instead. For (D) Paenibacillus was grown in 0.5x Nutrient with 1% starch overnight and directly diluted 1/2x or 1/10x into the same medium with additional 1g/L* NH_4Cl*. The bacteria were grown at 30°C. The plots show mean and SEM of three replicates each.*

Paenibacillus sp. growth at different pH values and its production of organic acids

Paenibacillus sp. was pre-cultured in tryptic soy broth. The next day it was diluted into 1xNu with 100mM Phosphate pH7 and grown to OD2. After washing three times in Base medium with 10mM Phosphate the bacteria were adjusted to an OD of 2 and diluted 1/100x into Base medium with 100mM Phosphate with the pH ranging from 3 to 7. The CFU was measured at the beginning and after 24hours to obtaine a fold growth of the bacteria. As can be seen in Fig. S1A *Paenibacillus sp. c*annot grow at low pH values. This is in line with Fig. 1 where upon reaching a pH of around 5 the bacteria start to die and again shows that it is the pH that drive the ecological suicide.

To better understand how *Paenibacillus sp.* changes the pH of the medium we grew it in M9 buffer with 2 % Glucose as only carbon source. After 24hours the spent medium was analyzed with mass spectrometry. As can be seen in Fig. S1B a variety of organic acids could either be found to increase in concentration or to become detectable at all.

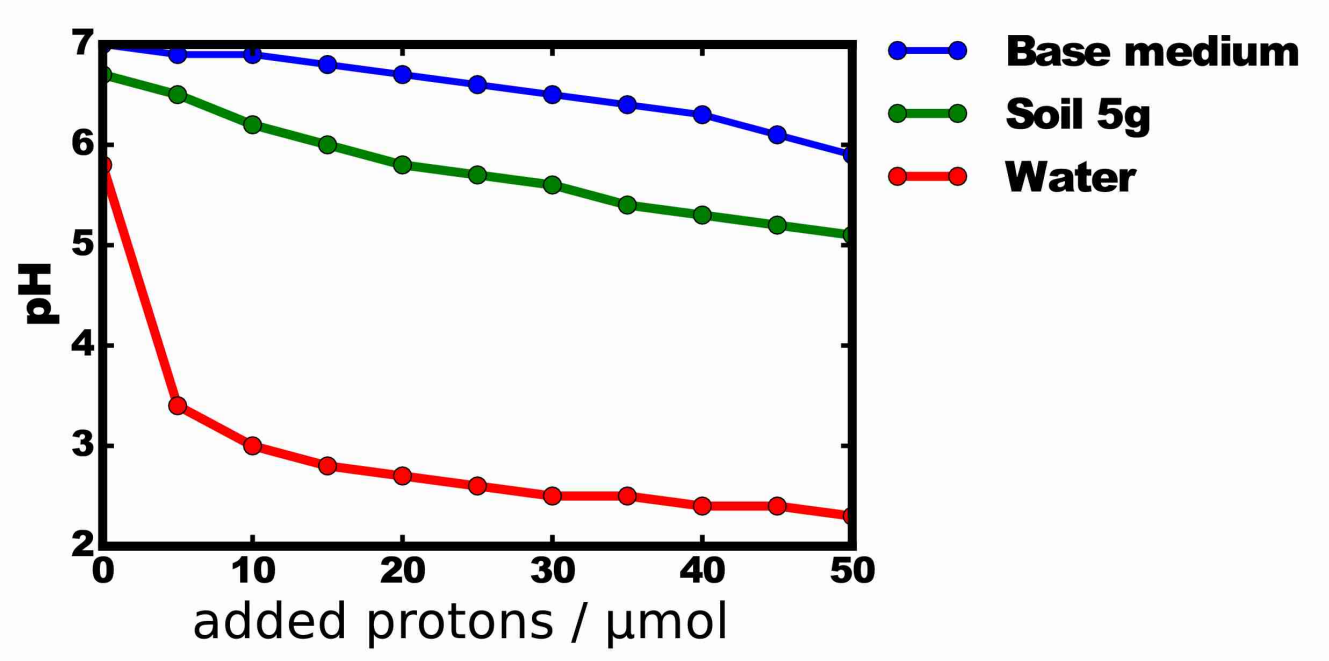

Supplementary Fig. 2: Buffer capacity of Base medium with 10mM Phosphate is higher than that of the soil the microbes were isolated from. *5g (wet weight) soil from the same location the microbes of this study were isolated from was dispersed in 15mL water. The pH of this dispersion was measured while hydrochloric acid was added. The obtained titration curve was compared with that of 5mL Base medium and pure water. As can be seen our medium is slightly stronger buffered than the soil.*

The proton concentration in a buffer system is given by:

$$H = \frac{K_d HA}{A}$$

with H as proton concentration, K_d as the dissociation constant and A as the base concentration. This can be converted by canceling out the volume into

$$H = \frac{K_d n_{HA}}{n_A}$$

Upon adding a small amount hydrochloric acid n_{HCl} this acid reacts with the acid and base present such that:

$$H_{new} = \frac{K_d (n_{HA} + n_{HCl})}{n_A - n_{HCl}}$$

from which the buffer capacity will be obtained as

$$\frac{-\log(H_{new}) + \log(H_{old})}{\Delta n_{HCl}}$$

Thus the buffer capacity is independent from the volume (and thus the soil can be diluted with water without affecting the buffer capacity) but just depends on the total amount of buffer, therefore the initial volume/mass for all samples was 5mL/5g.

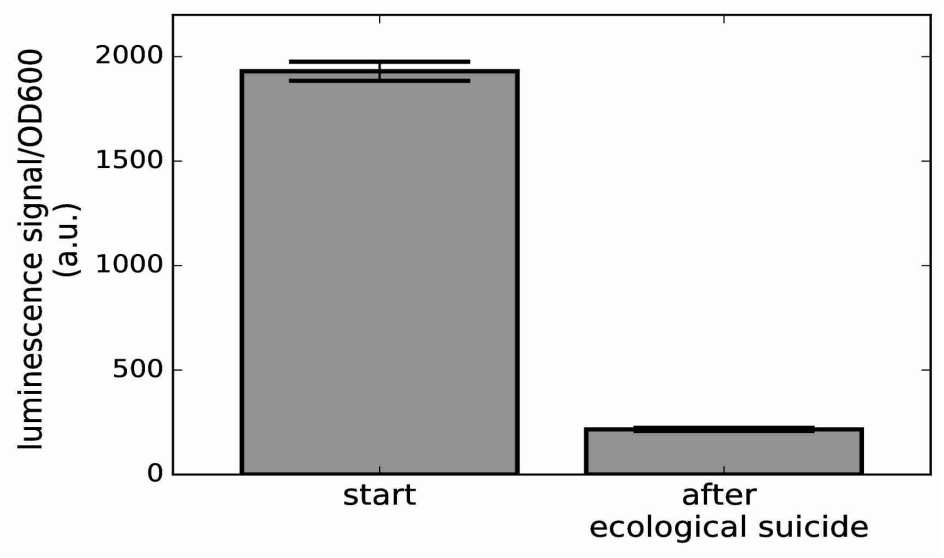

Supplementary Fig. 3: Cell viability assay confirms loss of viability upon ecological suicide. The BacTiter-Glo (Promega, Madison, USA) assay was used that measured the cellular ATP content as a indicator for cell viability. As all cell viability assays also this one has the disadvantage that cellular ATP levels to not have to be directly linked to cell viability. However, upon ecological suicide a drop of cellular ATP levels of around 90% could be observed. The final values were taken after 24hours in Base medium with 10mM Phosphate and 10g/L glucose. Bars show mean of 4 replicates and error bars show SEM.

Dependence of the nanobeads' fluorescence intensity on the pH:

To study the dynamics of the pH, we fabricated fluorescent nanobeads (see methods) which show a pH-dependent fluorescence intensity [3]. These nanobeads contain fluorescein, whose fluorescence intensity depends on the pH, and a highly photostable fluorinated porphyrin (TFPP), which acts as a red-emitting

pH independent reference dye. Since the fluorescence intensity of TFPP is independent of pH it serves as internal standard to make the result independent of the overall nanobead concentration. Thus, the ratio of the fluorescein and TFPP fluorescence signals is a function only of the pH value. Since in our 24-hours experiments the pH varied between 4 and 7, we measured the fluorescence intensity ratio of the nanobeads for different pH values in this range. The fluorescence intensity ratio increases monotonic for increasing pH. Moreover, the slope of the intensity ratio decreases for decreasing pH and the intensity seems to saturate for low pH (Fig. S4).

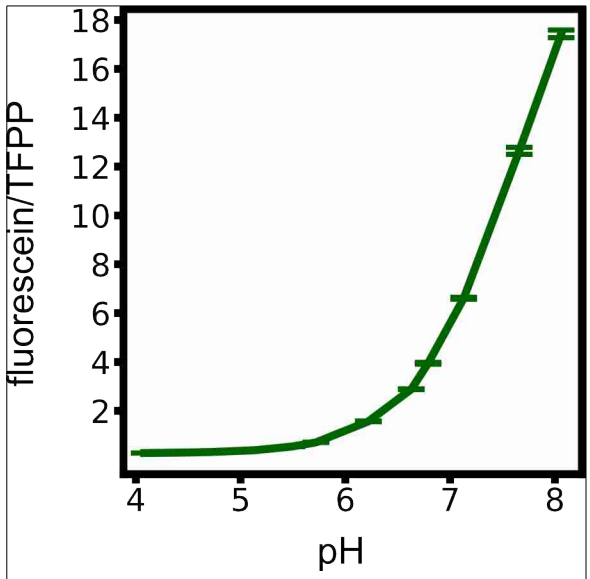

Supplementary Fig. 4: The nanobeads' fluorescence ratio of fluorescein and TFPP depends on the pH. *Rescaling the fluorescein signal with the TFPP signal shows a monotonic increase as a function of the pH. The fluorescence of the nanobeads was measured in base medium with adjusted pH values as shown on the x-axis. Errorbars show the SEM of 8 independent replicates.*

Dynamic measurements of the optical density and pH:

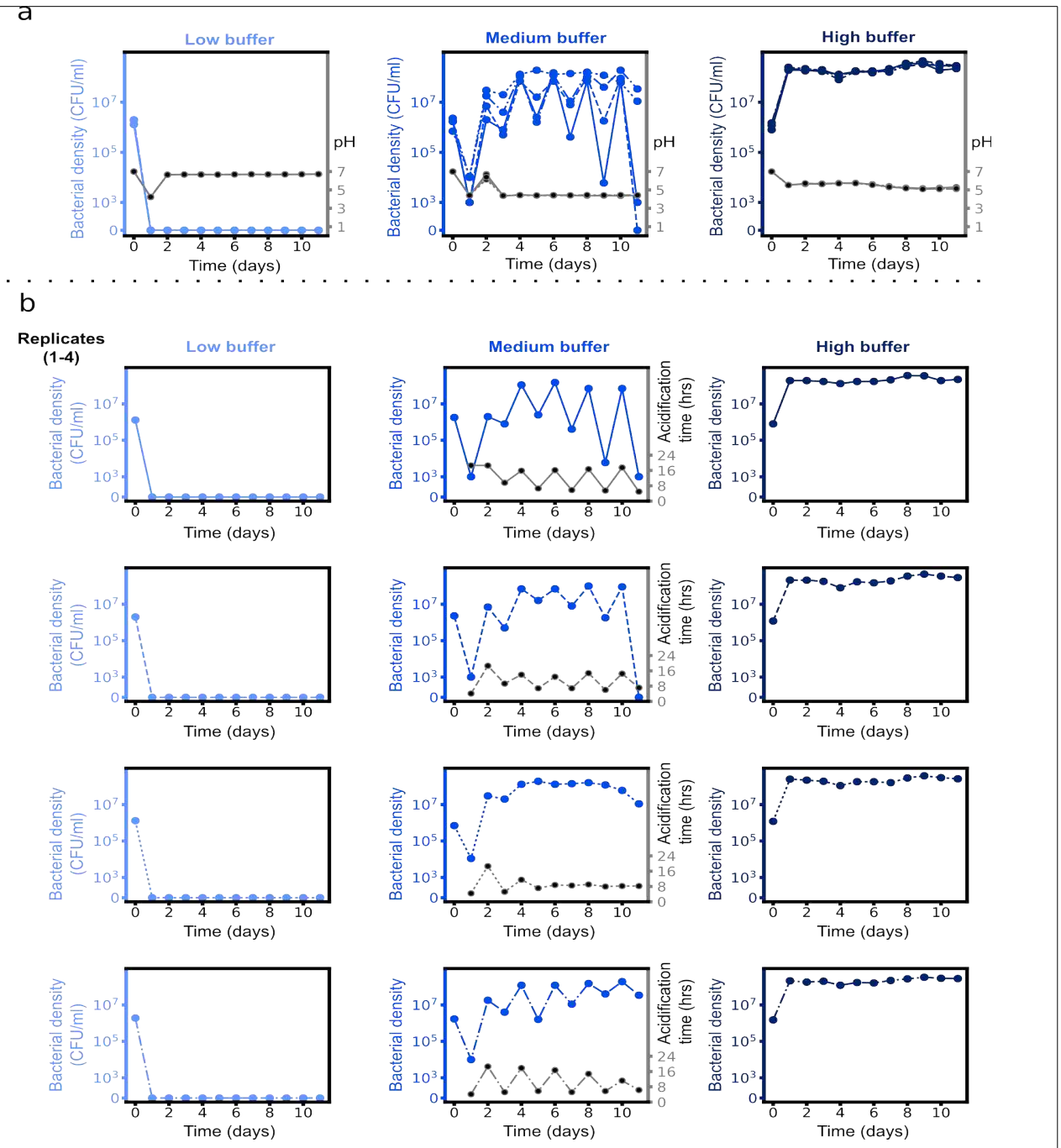

Supplementary Fig. 5: Population oscillations. *(a) Independent of the initial bacterial density, the daily final pH saturates at the same values. The four blue lines in (c-e) (solid, dashed, dotted, dashed-dotted) show the respective replica also shown in Fig. 2c-e. Instead of the acidification time we plot here the respective daily final pH values in grey (replicates are hardly distinguishable and the daily final pH of the replica are nearly identical). (b) Replicates of Fig. 2 c,d,e as separate plots.*

As detailed in the main text (Fig. 2c-e), our daily dilution experiments show oscillatory behavior of the bacterial density, which was measured at the end of each day. In contrast, we could not observe significant oscillations in the pH at the end of each day, i.e. for a certain buffer concentration, the pH after one day was approximately constant (Fig. S5).

This suggests that from the pH values at the end of each day it is not possible to infer the (oscillating) behavior of the bacterial density. Therefore, we also studied the dynamics of the pH during the course of each day during our daily dilution experiment. To this end, we prepared parallel experiments with the same buffer conditions and initial bacterial dilutions as for the daily dilution experiments (see Methods). In contrast to the daily dilution experiments, to these parallel experiments we also added fluorescent nanobeads and measured the optical density and fluorescence intensity of the nanobeads (see Methods). Whereas for the bacterial density (CFU/ml) at the end of each day we counted the living bacteria, the optical density provides a measurement for the total amount of bacteria (dead and alive). As detailed above (Fig. S4), the fluorescence intensity ratio of the nanobeads provides a measure for the pH.

For very low buffer concentrations (10mM phosphate), our daily dilution experiments (Fig. 2 left) display ecological suicide during the first day already. Consistently, in the corresponding parallel experiment with fluorescent nanobeads we find an early and strong decrease of the fluorescence intensity ratio after four hours of the first day already, indicating a strong decrease in pH (Fig. S6). This drop in pH is accompanied by a rapid increase of the optical density. On the second day (and all following days), the optical density mostly stays constant for the entire day. This strongly suggests that the bacteria have died on the first day already, which is underlined by finding no viable cells via plating on rich medium agar (Fig. 2c). In all measurements of the nanobeads' intensity ratio, we find an initial rapid increase. We argue that this initial increase is due to the initial increase in temperature during the

initial heating of the PlateReader to 30°C. When suspended in pure base (without bacteria) we indeed observed an increase of the fluorescence signal of the nanobeads for increasing temperature (Fig. S7).

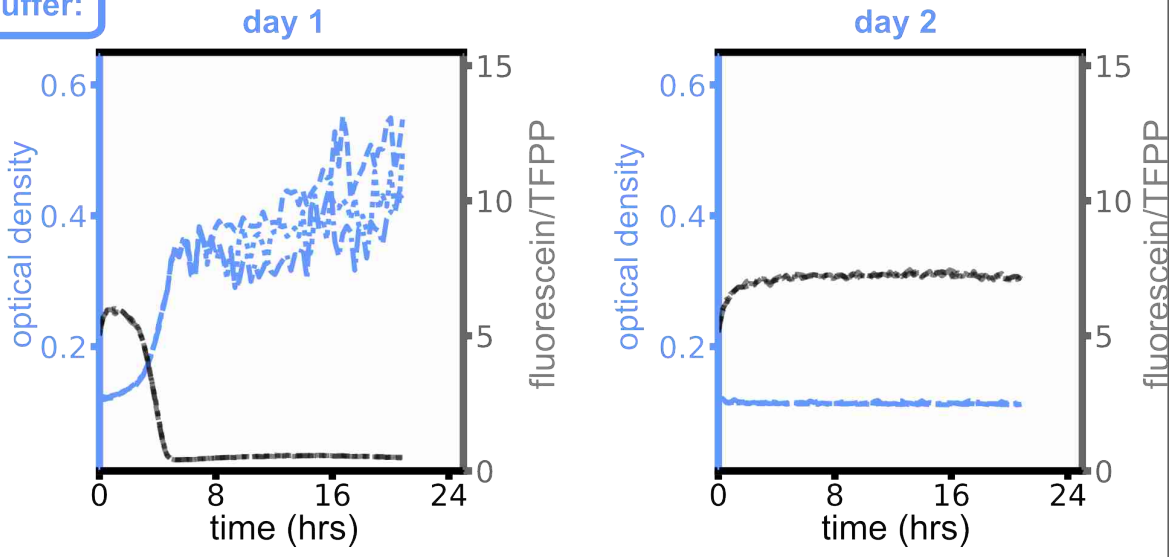

Supplementary Fig. 6: For low buffer concentrations (10mM phosphate), an early pH drop leads to ecological suicide. *The three sample curves (dashed, dotted, dotted-dashed) correspond to the samples of the daily dilution experiment in Fig. 2 of the main text for the first two days. The fluorescence intensity of fluorescein/TFPP drops after four hours already, eventually leading to ecological suicide on the first day. There was no background correction for the OD values which explains the nonzero OD on day 2.*

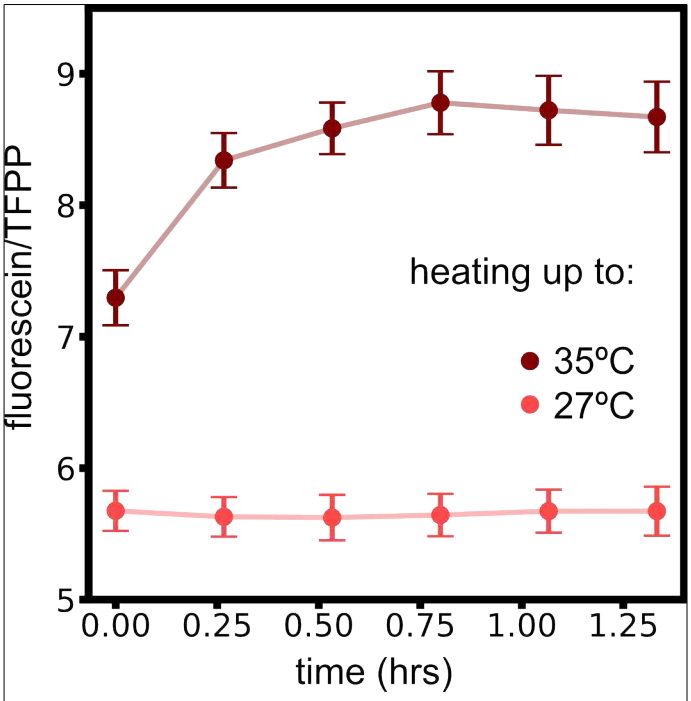

Supplementary Fig. 7: The fluorescence intensity ratio of the nanobeads is temperature dependent. *The temperature dependence rationalizes the initial increase of the fluorescence intensity ratio in Supplementary Fig. 6 and 8. The fluorescence of the nanobeads was measured over time in base buffer at pH 7. First the nanobeads were incubated at 27°C until a stable value could be obtained. Afterwards the temperature was increased to 35°C and the measurement continued. The increase in temperature is followed by a increase in the fluorescence ratio, which shows that the signal is temperature dependent. Mean and SEM of 10 replicates are shown.*

For high buffer concentrations, the optical density and the nanobeads' fluorescence intensity show a similar respective increase or decrease on each day (Fig. S8 a,c). This is consistent with the daily saturation of the bacterial density observed in our daily dilution experiments (Fig. 2e). As mentioned

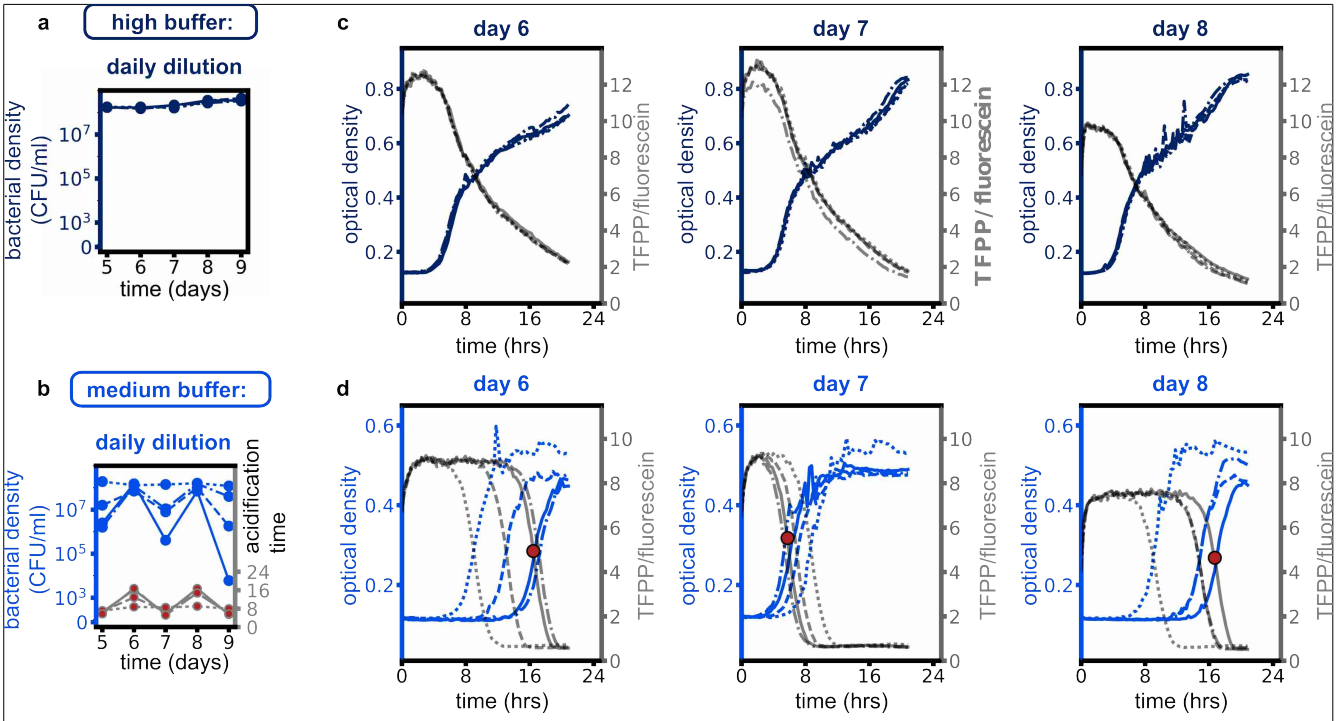

Supplementary Fig. 8: The acidification time oscillates with the bacterial density. (a-b) *The daily dilution experiments for high (100mM phosphate) and medium (26mM phosphate) buffer concentrations show daily saturation and oscillatory behavior of the bacterial density, respectively.* ***(c)*** *For high buffer concentrations, the fluorescence intensity and the optical density in the parallel experiments with fluorescent nanobeads show similar dynamics each day.* ***(d)*** *In contrast, for medium buffer concentrations the corresponding parallel experiments with fluorescent nanobeads reveal oscillations in the acidification time (red circle, shown for one sample represented by the solid line). The four different replica (solid, dotted, dashed, dotted-dashed) of these parallel experiments correspond to the respective replica shown in Fig. 2c-e.*

above, for intermediate buffer concentrations we could observe oscillations in the bacterial density but not in the pH at the end of each day (Fig. S5). However, our parallel experiments with fluorescent

nanobeads reveal oscillatory behavior of the time the fluorescence intensity--and thus also the pH--drops (acidification time, which is defined as the turning point of the resulting S-shaped fluorescence ratio curve). A late drop of the fluorescence is accompanied with a high final bacterial density in the daily dilution experiment and an early drop with a low final bacterial density. Hence, for intermediate buffer concentration the acidification time in our parallel experiment oscillates with the bacterial density in the daily dilution experiment (Fig. S8).

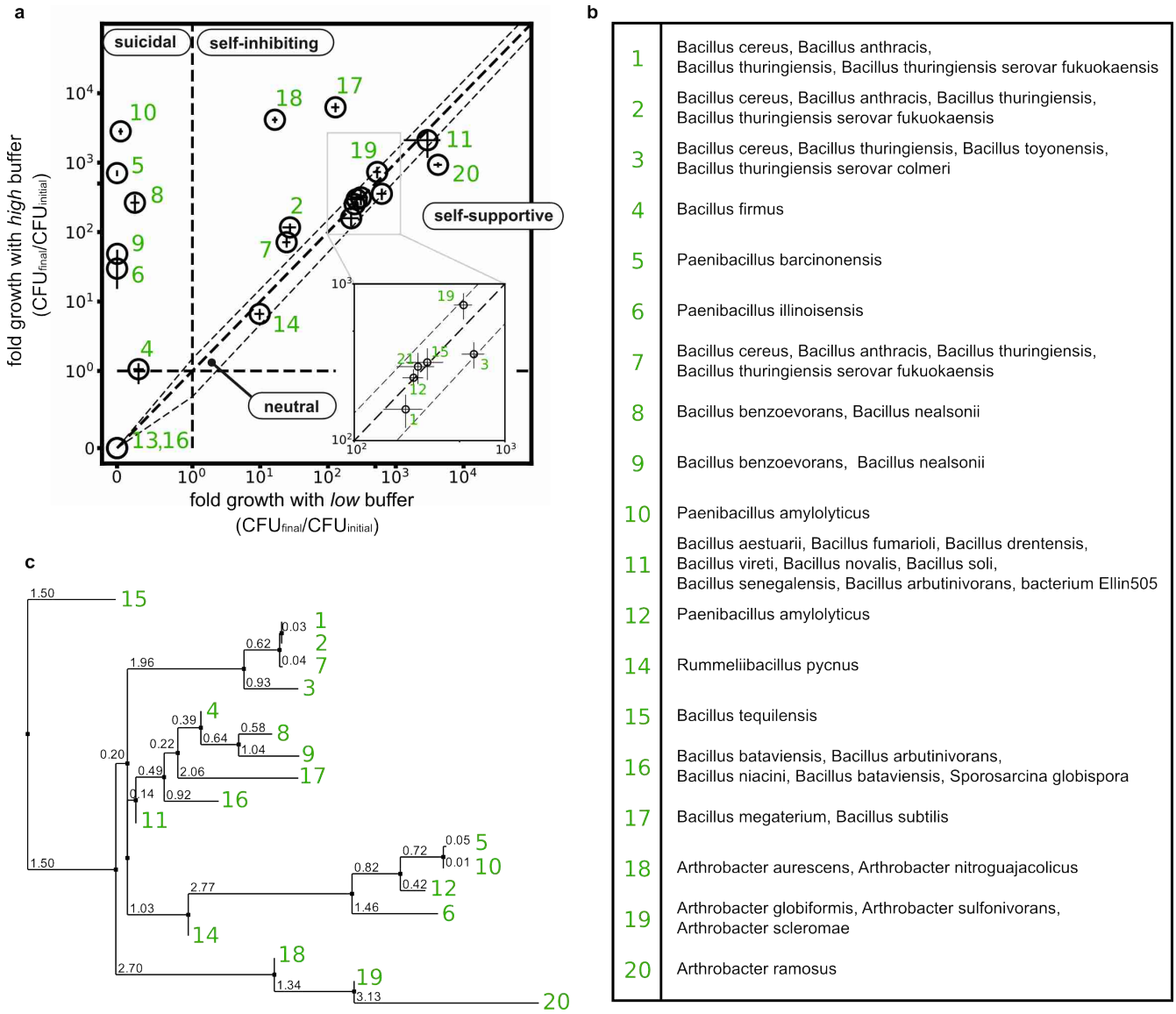

Supplementary Fig. 9: Relatedness of the used soil bacteria used to study the frequency of ecological suicide (Fig. 4 in main text) *(a) Categorization of the studied soil species as in Fig.4. The green numbers assign the individual species to their position in the phylogenetic tree (c). (b) Identification of the used species based on their 16s rRNA sequence according to RDB/SeqMatch tool [2]. The right column lists all respective related bacteria with maximal similarity score and S_ab score. (Sequencing of species 13 and 21 failed.) (c) Phylogenetic tree which shows the relatedness of the used bacteria. Green numbers stand for the species used in (a) and assigned in (b), black numbers show genetic distance. The* similarity matrix was calculated from the percentage identity (PID) between the sequences after multiple sequence alignment. The tree was build by neighbor joining method [8].

Mathematical approach to ecological suicide**:**

As detailed in the main text, our conceptual understanding of ecological suicide is based on the following principles: bacterial growth leads to a change in their environment (pH) in a way that eventually harms themselves and leads to their own death. Hence, bacteria experience a negative feedback mediated by the surrounding pH. It is important to note that we do not seek a complete description of ecological suicide including all the molecular details, but rather want to test our conceptual understanding (negative feedback) on a phenomenological level. Here, we show that from a mathematical perspective, ecological suicide is a very generic phenomenon, which can be captured by a minimal extension of previous mathematical descriptions of bacterial growth [5]. Bacteria have an optimal pH value where they grow best [8,9]. Deviations from this value deteriorate their growth and can even cause their extinction. To account for this pH dependence of bacterial growth, we propose the following dynamics for the bacterial density n:

$$\frac{dn}{dt} = \alpha n \left(1 - \frac{n}{\kappa}\right) \Gamma[p] \quad , \tag{1}$$

where α and κ are the growth rate and the carrying capacity, respectively, and the function $\Gamma[p]$ depends on the proton concentration p and represents the effect of the proton concentration (pH) on the bacterial growth. For a fixed $\Gamma[p]$, this equation is the well-studied logistic growth with growth rate $\alpha\Gamma[p]$ and carrying capacity κ . One ad hoc choice to account for a pH dependence of the bacterial growth is to assume that the deterioration of bacterial growth with changing proton concentration follows a Gaussian. Here, we define

$$\Gamma[p] := 1 - \left(\frac{1 - \exp\left[\frac{\left(p - p_{opt}\right)^2}{2\sigma^2} \right]}{1 - \exp\left[\frac{\left(p^c\right)^2}{2\sigma^2} \right]} \right) \quad , \tag{2}$$

where p_{opt} denotes the optimal proton concentration and p^c denotes some critical proton concentration deviation beyond which bacteria start to die. All of these proton concentrations are not in physical units but instead is simply meant to capture the dynamics of the proton concentration. σ determines how far from the optimal proton concentration the species can grow / survive. Based on the strong correlation between the increase in the optical density and the fluorescence intensity ratio (Fig. S6 and S8), we assume that the change in pH—and thus the proton concentration—is directly related to the growth of the bacteria. A naive assumption would therefore be that the change in proton concentration is simply proportional to the change in bacterial density and is completely determined by eq. (1). However, note that in this case the system reduces to a system of only one dynamic variable (the bacterial density n) which would not be able to reproduce non-monotonic growth [39] as observed in our experiments (Fig. 1). There are many ways to implement a negative feedback of the proton concentration on the bacterial density capable of reproducing non-monotonic behavior as observed in our experiments [4,5]. The goal of our mathematical description is not to account for the molecular details of the process, which would involve the complex (and largely unexplored) metabolism of the particular bacteria under consideration (in our case *Paenibacillus sp*.). In contrast, our goal is to develop a simple mathematical model that delivers intuition about the dynamics of ecological suicide in *Paenibacillus sp.* and test its consequences especially in the light of the experimental findings like non-montonous growth and oscillations.

Fig. 1c displays a decrease of the pH even after saturation of the bacterial density and thereby suggests, that the proton concentration also couples to the bacterial density itself. Since, in principle, the proton concentration could depend on both the change of the bacterial density $\left(\frac{dn}{dt}\right)$ and the bacterial density (n) itself, we make the following approach for the dynamics of p :

$$\frac{dp}{dt} = \beta_1 \left(\frac{dn}{dt} \right) \Theta \left[\frac{dn}{dt} \right] + \beta_2 n, \tag{3}$$

where β_1 and β_2 are (real, positive) coupling parameters. $\Theta[\cdot]$ denotes the Heaviside step function, which is one for a positive argument and zero otherwise and accounts for our assumption that bacteria increase the proton concentration during their growth, but do not affect the pH when they die. Whereas high β_1 and β_2 will yield a fast increase in the proton concentration with bacterial growth and total density respectively, for very low β_1 and β_2 the proton concentration will hardly change. We therefore assume a decrease of β_1 and β_2 to emulate an increase in buffer concentration in our experiments. This model is thus an extension of the simpler model used in [10]. Measuring time, bacterial density and proton concentration in units of $1/\alpha$, κ, and p_{opt}, respectively, the only independent parameters are the rescaled coefficients coupling p to $\frac{dn}{dt}$ and n given by $\beta_1' = \beta_1 \kappa / p_{opt}$ and $\beta_2' = \beta_2 \kappa / (\alpha\, p_{opt})$, respectively, the rescaled critical proton concentration deviation p^c / p_{opt}, and the rescaled spread σ / p_{opt}. Fig. S10 a-c show the dynamics of the bacterial density and the proton concentration as a function of time for a certain time interval $24/\alpha$,which is proposed to simulate daily growth. In all simulations we chose the same values for $p^c / p_{opt} = 0.6$ and $\sigma^2 / p^2_{opt} = 1$, assumed the initial proton concentration to be optimal and only varied the coupling coefficients β_1' and β_2'. For convenience, the proton concentration is plotted as $-\log(p)$, which is up to some scaling the corresponding pH of the system. Similar to our experimental observations for increasing the buffer concentration (compare to Fig.1 a-c), decreasing the coupling of the proton concentration to the bacterial density (by lowering β_1' and β_2') shows a transition from a rapid decline of the bacterial density for strong coupling to saturation of the bacterial density at the carrying capacity for weak coupling (Fig. S10 a-c). Note, that due to the continuous

description, the bacterial density n cannot reach 0 (extinction) but only approaches 0 at infinite times. However, from our daily dilution experiments (Fig. 1c) we can estimate the carrying capacity with approximately 10^8 cells; hence bacterial densities below $1/10^8\kappa$ would correspond to less than one cell. We therefore claim that bacterial densities below $1/10^8\kappa$ correspond to extinction in our experiments and manually set the bacterial density to zero, if it is lower than $1/10^8\kappa$. Starting at different initial conditions, the fold growth of the bacteria is decreasing for increasing initial concentrations (Fig. S10 d), as observed in our experiments (Fig. 2a). Similarly, there is a critical maximal initial density above which the bacteria start to die out (the fold growth drops below 1). Eqs. (1)-(3) were solved for different initial bacterial densities and proton concentrations as well as different rescaled coupling coefficients $\beta_1^{'}$ and $\beta_2^{'}$ using NDsolve[] in Wolfram Mathematica 11. Similar to our experiments, this reciprocal dependence of the initial to the final density leads to interesting behavior when simulated in a "daily dilution" simulation: Here, we numerically integrated equations (1) to (3) for $24/\alpha$, which in line with our above simulations represents one day of our experiments. To account for the 1/100x daily dilution, the final bacterial concentration is multiplied by a factor of 1/100 and then taken as the initial bacterial density of the subsequent simulation. Note, that this procedure can be understood as a discrete map for the bacterial density, where - apart from the dilution factor of 1/100 - the mapping is given by the relation of the bacterial density at t= $24/\alpha$ and $t=0$ as given in Fig. S6d. Discrete maps show a rich phenomenology ranging from stable fixed points and limit cycles to chaos and can be very sensitive to the form of the mapping function [6]. Similarly, we expect that changing the form of the mapping function (Fig. S10 d) by changing the coupling constants $\beta_1^{'}$ and $\beta_2^{'}$ is critical for the long-term behavior in our daily dilution simulations. In view of the similar shapes of this mapping (Fig. S10 d) and the well-studied logistic map [7]we speculate that for a very shallow shape--as it occurs for weak coupling (small $\beta_1^{'}$ and $\beta_2^{'}$)--the discrete map approaches a stable fixed point, whereas for a steep (negative) slope due to strong coupling (large

β_1' and β_2') the bacterial density will diverge until it eventually takes values below $1/10^8 \kappa$ (extinction). For intermediate slopes, i.e. for intermediate values for β_1' and β_2' , the daily dilution simulations may show oscillations between multiple values (Fig. S10 g). Fig. S11 shows respective bifurcation diagrams of our daily dilution simulations when varying the coupling constants β_1' and β_2' continuously. These bifurcation diagrams display bifurcations from one stable fixed point to oscillations between two values of the bacterial density. Also our experiments suggest bifurcations between a fixed final bacterial density and oscillations between multiple values (Fig. S12). Due to the sensitivity of logistic maps against a change in the mapping function and due to natural noise in our experiments, we note however that a quantitative categorization of the oscillations observed in our experiments (Fig. 2d) in terms of limit cycles of the underlying discrete map (Fig. 2a) may not be feasible and is beyond the scope of this work.

In our daily dilution simulations, for very strong coupling of the proton concentration to the bacterial density ($\beta_1'=3, \beta_2'=1$), the bacterial density dramatically decreases on the first "simulation day" already (Fig. S10 f). Due to our continuous description, the bacterial density does not reach zero. However, note that the bacterial density drops below $1/10^8 \kappa$, which corresponds to extinction as detailed above (to account for this extinction, we therefore manually set the density to zero). For medium coupling ($\beta_1'=0.3, \beta_2'=0.1$), we find oscillations in the final bacterial density (Fig. S10 g), reminiscent to our daily dilution experiments with intermediate buffer concentration (Fig. 2d). Furthermore, we find, that the acidification time (the time of the turning point in the proton concentration) oscillates with the bacterial density. For weak coupling ($\beta_1'=0.06, \beta_2'=0.02$), the bacterial density saturates at the carrying capacity after the first day already and all subsequent "simulation days" (Fig. S10 h), as observed in our experiments with high buffer concentration (Fig. 2e). The phenomenological agreement between our mathematical description and our experiments strongly

suggests, that the coupling of the bacterial density and the environment (here the pH) and the resulting non-monotonic growth dynamics are key aspects in understanding the phenomenon of ecological suicide.

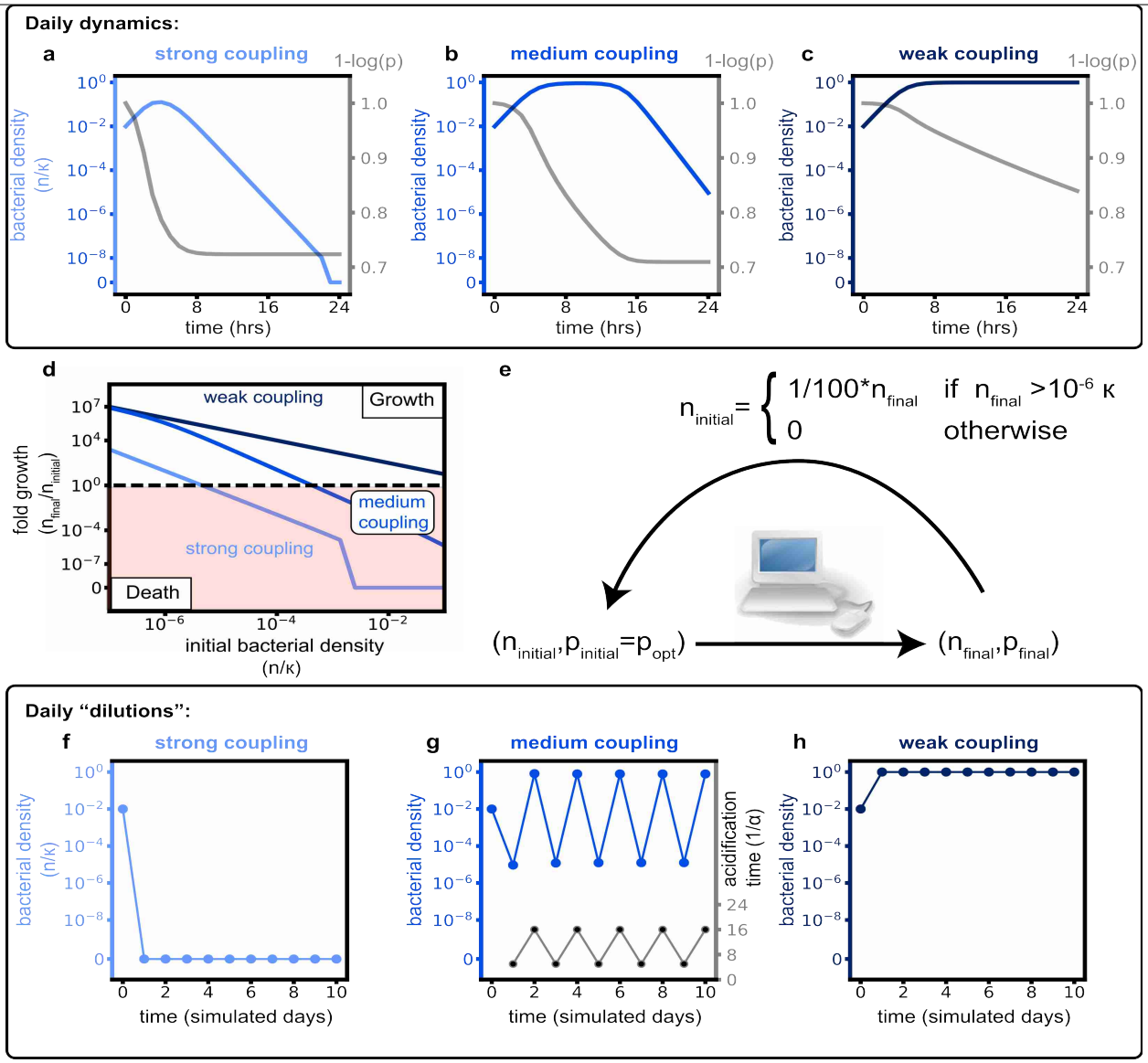

Supplementary Fig. 10: Negative feedback of the pH on the bacterial density suffices to recapitulate the phenomenology of ecological suicide as observed experimentally. a-c, Based on eq. (1)-(3), strong ($\beta_1'=3, \beta_2'=1$), medium ($\beta_1'=0.24, \beta_2'=0.08$), and weak ($\beta_1'=0.06, \beta_2'=0.02$ coupling has a similar effect on the growth dynamics as low, medium and high buffer concentrations in our experiments (Fig. 2c-e). **d,** The fold bacterial growth decreases for increasing initial concentration. When simulated in a "daily dilution" scheme. If the cell number that is 'diluted' at the end of the day dropped below one cell – this is possible since the variables are continuous in differential equitations -the bacterial density was set to zero. **e**, this reciprocal dependence leads to similar scenarios, **f-h,** as observed experimentally (Fig. 2, c-e).

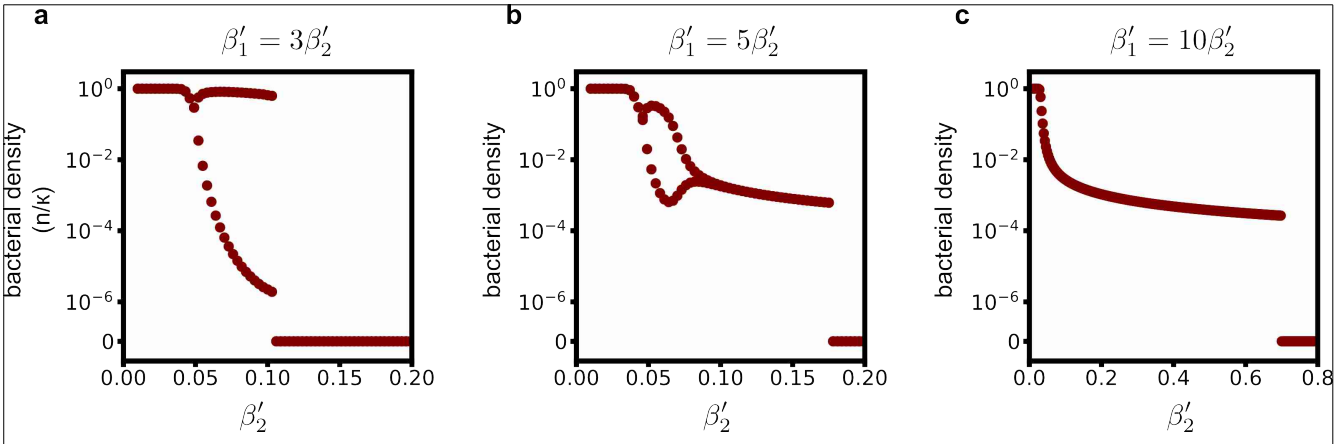

Supplementary Fig. 11: Varying the coupling constants β_1' and β_1' shows bifurcations from one fixed point to oscillations between two points. The bifurcation diagrams show the values of the bacterial density at the end of the last two days after 'daily dilution' simulations corresponding to 60 days. **a,** For comparable coupling constants (here: $\beta_1'=3\beta_2'$, as used in Fig. S6), the discrete mapping of 'daily dilution' simulations displays a bifurcation from one stable fixed point (saturation) to oscillations between two points. When a 1/100 dilution would cross the cutoff of $1/10^8\kappa$ (i.e. if after any of the 60 simulation days $n<1/10^6\kappa$), the bacterial density was manually set to zero. **b,** For an intermediate ratio $\beta_1'/\beta_2'=5$, the amplitude of oscillations first increases and then decreases again for increasing β_2' . **c**, For high enough β_1'/β_2' (here: $\beta_1'/\beta_2'=5$) the coupling to the change of bacterial density is dominant and the system saturates at low final densities, but shows no oscillations (recall that strong enough coupling to the bacterial density itself is crucial in our equations (3) to generate oscillations). In b, and c, the bacterial density drops below the extinction cutoff after the first first day already when β_2' is too high.

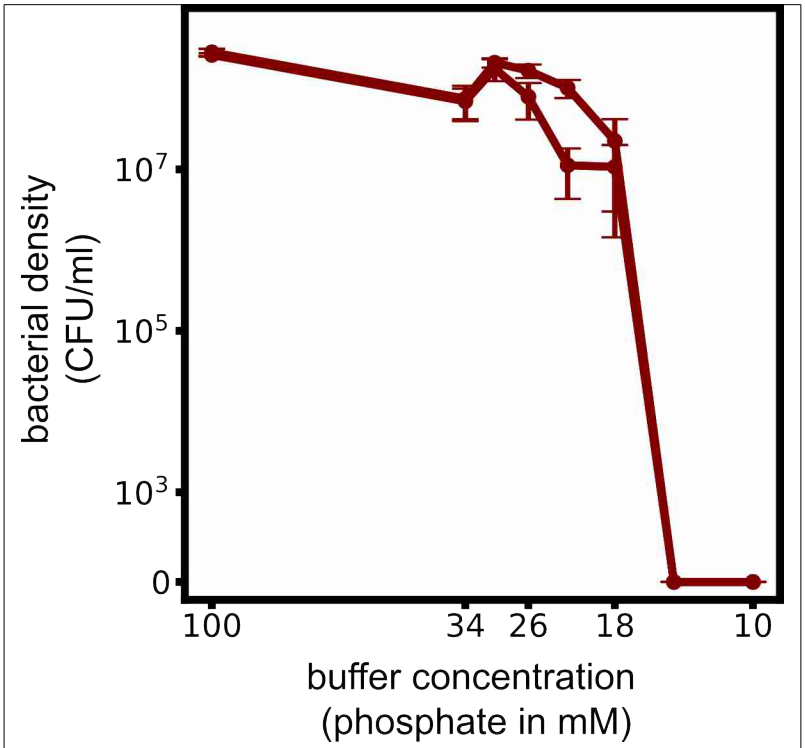

Supplementary Fig. 12: Experiments suggest a bifurcation between stable bacterial density at the end of each day and oscillations. The 'bifurcation diagram' shows the mean amplitude of the final bacterial density on the last day (day 11) and the second last day (day 10) for different buffer concentrations. The mean and SEM of the 4 replicates also used in Fig. 2 are shown.

References:

1. Nelson, D. M., Glawe, A. J., Labeda, D. P., Cann, I. K. O. & Mackie, R. I. Paenibacillus tundrae sp. nov. and Paenibacillus xylanexedens sp. nov., psychrotolerant, xylan-degrading bacteria from Alaskan tundra. *Int. J. Syst. Evol. Microbiol.* **59,** 1708–1714 (2009).

2. Cole, J. R. *et al.* Ribosomal Database Project: data and tools for high throughput rRNA analysis. *Nucleic Acids Res.* **42,** D633–D642 (2014).
3. Wang, X., Meier, R. J. & Wolfbeis, O. S. Fluorescent pH-Sensitive Nanoparticles in an Agarose Matrix for Imaging of Bacterial Growth and Metabolism. *Angew. Chem. Int. Ed.* **52,** 406–409 (2013).
4. Strogatz, S. H. *Nonlinear Dynamics and Chaos: With Applications to Physics, Biology, Chemistry, and Engineering*. (Westview Press, 2014).
5. May, R. M., Conway, G. R., Hassell, M. P. & Southwood, T. R. E. Time Delays, Density-Dependence and Single-Species Oscillations. *J. Anim. Ecol.* **43,** 747–770 (1974).
6. Hilborn, R. C. *Chaos and Nonlinear Dynamics: An Introduction for Scientists and Engineers*. (Oxford University Press, 2000).
7. May, R. M. & others. Simple mathematical models with very complicated dynamics. *Nature* **261,** 459–467 (1976).
8. Saitou, N. & Nei, M. The neighbor-joining method: a new method for reconstructing phylogenetic trees. *Mol. Biol. Evol.* **4,** 406–425 (1987).
9. Basan, M. *et al.* Overflow metabolism in *Escherichia coli* results from efficient proteome allocation. *Nature* **528,** 99 (2015).